Fermi National Accelerator Laboratory

FERMILAB-Pub-90/167-A
August 1990

STOCHASTIC INFLATION AND NONLINEAR GRAVITY

D.S. Salopek
NASA/ Fermilab Astrophysics Center
P.O. 500 MS-209, Batavia, Illinois, USA 60510

J.R. Bond
CIAR Program, Canadian Institute for Theoretical Astrophysics,
University of Toronto, Toronto, Canada M5S 1A1

Abstract:

We show how nonlinear effects of the metric and scalar fields may be included in stochastic inflation. Our formalism can be applied to non-Gaussian fluctuation models for galaxy formation. Fluctuations with wavelengths larger than the horizon length are governed by a network of Langevin equations for the physical fields. Stochastic noise terms arise from quantum fluctuations that are assumed to become classical at horizon crossing and which then contribute to the background. Using Hamilton-Jacobi methods, we solve the ADM constraint equations which allows us to separate the growing modes from the decaying ones in the drift phase following each stochastic impulse. We argue that the most reasonable choice of time hypersurfaces for the Langevin system during inflation is $T = \ln(Ha)$, where H and a are the local values of the Hubble parameter and the scale factor, since T is the natural time for evolving the short wavelength scalar field fluctuations in an inhomogeneous background. We derive a Fokker-Planck equation which describes how the probability distribution of scalar field values at a given spatial point evolves in T. Analytic Green's function solutions obtained for a single scalar field self-interacting through an exponential potential are used to demonstrate: (1) If the initial condition of the Hubble parameter is chosen to be consistent with microwave background limits, $H(\phi_0)/m_p \lesssim 10^{-5}$, then the fluctuations obey Gaussian statistics to a high precision, independent of the time hypersurface choice and operator ordering ambiguities in the Fokker-Planck equation. (2) For scales much larger than our present observable patch of the Universe, the distribution is non-Gaussian, with a tail extending to large energy densities; although there are no observable manifestations, it does show eternal inflation. Lattice simulations of our Langevin network for the exponential potential demonstrate how spatial correlations are incorporated. An initially homogeneous and isotropic lattice develops fluctuations as more and more quantum fluctuation modes leave the horizon, yielding Gaussian contour maps for a region corresponding to our observable patch and non-Gaussian contour maps for the ultra-large scale structure of the Universe. Inflation models with extended non-Gaussian tails at observable scales would lead to a radically different cosmic structure than Gaussian perturbations give.

Submitted to Phys. Rev. D

I. INTRODUCTION

One of the most important problems in inflation cosmology is to formulate the generation of density fluctuations for galaxy formation within a fully quantum mechanical framework including gravitational effects. Improvements in the current calculational methods would allow one to compute primordial fluctuations which are not described by Gaussian scale-invariant random fields. Modifications of the standard inflation model of structure formation, the adiabatic Gaussian scale-invariant Cold Dark Matter model, may be desirable for explaining large scale structure observations.[1-5] Techniques for performing inflation calculations include: (1) Using the quantum mechanical Wheeler-deWitt equation, one solves for the wavefunction of a homogeneous universe with linear perturbations,[6,7] but with no back-reaction of the perturbations on the homogeneous background. (2) Fluctuations of the metric and scalar fields are treated in linear perturbation theory as quantum Heisenberg operators on a homogeneous classical background,[8] again with no back-reaction; this method is well-suited for numerical calculations, because the quantum perturbation equations are almost identical to the classical perturbation equations.

We explore a different facet of the problem by considering a classical, inhomogeneous and nonlinear background which fluctuates only on scales larger than the Hubble radius. In the stochastic inflation framework developed by Vilenkin,[9] Starobinski[10] and many others, small scale quantum fluctuations are assumed to become classical upon horizon crossing and act as a stochastic force on the background. The fields are decomposed into long and short wavelength components,

$$\phi_j(t,x^i) = \bar{\phi}_j(t,x^i) + \delta\phi_j(t,x^i), \quad g_{\mu\nu}(t,x^i) = \bar{g}_{\mu\nu}(t,x^i) + \delta g_{\mu\nu}(t,x^i), \tag{1.1}$$

where $\bar{\phi}_j$ contains all Fourier modes longer than the horizon length, $(k/a)^{-1} > H^{-1}$, (H is the Hubble parameter) and $\delta\phi_j$ contains all modes shorter than the horizon length. $\bar{\phi}_j$ is treated as a classical field. When the quantum fluctuations embodied in $\delta\phi_j$ leave the horizon, they too are treated as a random classical field. This assumption cannot be rigorously justified, although recent work in the quantum to classical transition using simplified toy models[11] makes it appear reasonable. From a practical point of view, one can argue that the fields evolve essentially classically at large wavelengths although, strictly speaking, there is no consistent quantum theory of long wavelength evolution.[12] In this paper, we shall include the classical metric back-reaction at long wavelengths.

Starobinski[10] considered a scalar field slowly rolling down a potential in a de Sitter background. Guided by intuition, he made numerous assumptions and approximations in order to obtain the following Fokker-Planck (FP) equation,

$$\frac{\partial}{\partial t}P(t,\phi) = \frac{1}{3H_0}\frac{\partial}{\partial\phi}\left(\frac{\partial V}{\partial\phi}P\right) + \frac{H_0^3}{8\pi^2}\frac{\partial^2 P}{\partial\phi^2}, \tag{1.2}$$

which is a diffusion-type partial differential equation describing the probability $P(t,\phi)$ of observing a scalar field value at time t. That the scalar field interacts through a potential $V(\phi)$, whereas the fixed de Sitter background is characterized by a constant Hubble parameter, H_0, is an inconsistency in this equation. Over the past few years, researchers have tried to justify as well as extend this formalism. Bardeen and Bublik[13] obtained a FP equation for the case where a scalar field was slowly rolling down a potential while its energy density was causing the Universe to inflate; they also numerically integrated it. Graziani and Olynyk[14] chose instead to integrate the Langevin equation for the scalar field value at a point, which is an ordinary differential equation containing a stochastic noise term. With a more careful treatment of the quantum noise term in the Langevin equation, Hosaya, Morikawa and Nakayama[15] were able to remove the slow-roll assumption. Nakao, Nambu and Sasaki[16] wrote the Langevin equations in

a de Sitter background as a series of first order differential equations which allows one to have stochastic noise terms in the scalar field momenta as well as the scalar field itself.

The effects of metric fluctuations were not discussed in the initial formulation of stochastic inflation. Goncharov, Linde, and Mukhanov[17] incorporated metric fluctuations in linear theory. We extend this work by including the possibly nonlinear back-reaction of the metric at long wavelengths. We also find that one must carefully consider the time parameter that appears in the FP equation for the probability function to be meaningful. Time specifies the hypersurface upon which to measure the fluctuations. For example, if one chooses ϕ as time then all fluctuations in ϕ are necessarily zero, but the fluctuations are still present — in $\alpha = \ln a$. The time hypersurface should be specified in terms of the physical variables, ϕ and α in this case.

Grinstein, Allen and Wise[18] and Kofman and Linde[19] were the first to consider whether non-Gaussian fluctuations could arise in inflation; they worked in the context of an axion model. Ortolan, Lucchin and Matarrese[20,21] considered the possibility that non-Gaussian fluctuations for galaxy formation might arise in stochastic inflation driven by an exponential potential. Using approximate solutions of the FP equation, they claimed that non-Gaussian fluctuations for structure formation were generic. Hodges[22] has given an argument suggesting that fluctuations are characteristically Gaussian for a $\lambda\phi^4/4$ potential. We produce exact Green's function solutions of the Fokker-Planck equation for inflation with an exponential potential which demonstrate that fluctuations of relevance for our observed patch of the Universe would be Gaussian, although non-Gaussian fluctuations are generic on ultra-large (unobservable) scales.

The stochastic approach developed here is not an end in itself, but is a framework for understanding the nonlinear interaction of the metric and scalar fields in inflation models. The long wavelength problem is one of the easiest nonlinear, inhomogeneous gravitational models where one can calculate the full back reaction of the metric including gravitational radiation.[23] The long-short split at the Hubble radius thus serves as a powerful calculational tool in inflation models. The stochastic approach allows one to model nonlinear mode-mode coupling between long and short wavelengths. It captures some quantum features by applying a probabilistic description. But, ultimately, the linear treatment of short wavelength fluctuations that we adopt here is suspect because one must eventually incorporate a short distance cutoff to the theory. It is quite possible that the assumed independent Gaussian noise terms which arise from a ground state in linear perturbation theory are not correct. More complicated ground state configurations could arise because of nonlinear effects at some scale, say the GUT scale or possibly the Planck scale. In this case, the stochastic formalism would serve as a transport theory of short scale quantum fluctuations to wavelengths longer than the Hubble radius.

In Sec. II.A, we present the long wavelength background equations, consisting of the energy and momentum constraints, and a set of first order evolution equations for the physical fields, φ_j, $\alpha = \ln a$ and their momenta $\Pi^{\varphi_j} = \dot{\phi}_j/N$, $H = \dot{\alpha}/N$. $N(t,x)$ is the lapse function and $a(t,x)$ is the local scale factor of the Universe. The evolution equations contain stochastic noise terms because quantum fluctuations contribute to the inhomogeneous background when their wavelength exceeds the horizon length. The constraints do not contain noise terms and they reduce to a single partial differential equation, the separated Hamilton-Jacobi equation for *homogeneous fields* which may be solved without reference to the other equations. A tremendous simplification occurs if the decaying mode is neglected, since one may then disregard the evolution equations for the momenta.

Specifying the time surface on which the stochastic forces act is a difficult issue. In Sec. II.B, we suggest $T = \ln(Ha)$ as the time variable. On this time hypersurface, one may solve analytically for short wavelength quantum modes on a long wavelength background. When the wavelength of a mode exceeds the Hubble radius, it acts as a stochastic force on the long wavelength background. Because of the matching of short wavelengths on to large wavelengths

when $k = (Ha) = e^T$, the stochastic method is slightly imprecise. For the case where fields evolve relatively slowly, this is not a problem. The stochastic force depends on the local value of the Hubble parameter, which can lead to non-Gaussian fluctuations as the system evolves. Non-Gaussian fluctuations can also arise from nonlinearities due to mode-mode coupling in the background evolution. The probability, $P(\phi_j|T)$, of observing scalar field values ϕ_j on a surface of uniform T is governed by a Fokker-Planck equation.

The initial conditions for stochastic inflation are well posed if one wishes to model structure in our observable Universe. One begins with an isotropic and homogeneous patch of the Universe. Inhomogeneities in the long wavelength background fields are subsequently produced by quantum Fourier modes that leave the horizon with a Gaussian distributed amplitude having a root-mean square dispersion given by the Hawking temperature: $[k^3/(2\pi^2)|\delta\phi(k)|^2]^{1/2} = H/(2\pi)$, as suggested in linear theory (see Salopek, Bond and Bardeen,[8] which we shall refer to as SBB).

In Sec. III, exact Green's function solutions describing the evolution of an initial delta-function distribution are obtained for the case of a single scalar field in an exponential potential. Green's functions are examples of limited statistics which contain much valuable information; they describe the distribution of scalar field values in a lattice which began homogeneously with $\phi_j = \phi_{j0}$. One can also determine a nonlinear quantity analogous to the fluctuation spectrum from the moments of the one-point distribution.

We follow the evolution a single scalar field in a 3-dimensional lattice in Sec. IV. Spatial correlations arise entirely from the quantum noise terms. When the initial Hubble parameter is of the order of the Planck scale, significant non-Gaussian fluctuations appear. Although we find the size of the lattice is much larger than our observable Universe, this model is one of simplest examples of non-Gaussian fluctuations arising in cosmology, and it illuminates more realistic models involving multiple scalar fields. Finally, in Sec. V, we summarize our results.

II. INCORPORATING GRAVITATIONAL FLUCTUATIONS INTO THE STOCHASTIC FORMALISM

The stochastic approach is an approximate method for performing inflation calculations which has some similarities mathematically to the WKB method for solving bound state problems in elementary quantum mechanics: there is a rapidly oscillating WKB solution at small distances which is matched onto an analytically tractable large distance solution. In inflation, however, large and short distance refers to long and short wavelength decompositions of the fields; and instead of the matching occurring at the boundary between the classically allowed and forbidden regions, it is now at the comoving Hubble radius, which is continuously shrinking in time. As well, in inflation, the long wavelength growing solution is selected while the decaying solution can be dropped, whereas in the bound state problem the opposite occurs. Matching short and long wavelength fields at the Hubble radius is facilitated by using the Hamilton-Jacobi formalism,[12] which naturally separates the growing and decaying modes. Also, numerical calculations we have performed using linear perturbation theory[8] show that matching is quite straightforward in situations where the fields are evolving relatively slowly.

In Sec. A, we develop the stochastic long wavelength dynamical equations and solve the long wavelength constraint equations using Hamilton-Jacobi theory. In Sec. B., we treat short wavelength fluctuations using linear perturbation theory about an inhomogeneous long wavelength background, a generalization of the standard previous calculations of quantum fluctuations on a homogeneous background, and show that a Fourier-type WKB solution is a good approximation for wavelengths much smaller than the Hubble radius. Although this approximation breaks down when the wavelength of a Fourier mode approaches the Hubble radius, we argue by analogy with the homogeneous case that the stochastic contributions to the long wavelength fields are adequate representations of the physics involved. This WKB approximation suggest a

natural choice for the time hypersurfaces for evolving the long wavelength fields: those on which the local conformal time τ is uniform. We also show that surfaces of constant comoving Hubble radius $(Ha)^{-1}$ are more tractable and yet provide reasonable approximations to the τ surfaces. In Sec. C, we derive the Langevin and Fokker-Planck equations for the long wavelength fields. In Sec. D, we discuss the form of the initial conditions for stochastic inflation. In Sec. E, we show how to transform the late time Fokker-Planck probability distribution to a form that may be compared with observations. A useful fluctuation function computable from the moments of the Green's function solution to the Fokker-Planck equation is introduced which provides a simple measure of the fluctuations as a function of physical volume.

A. Inhomogeneous Background Equations

We consider a system of real scalar fields, ϕ_j, $j = 1, n$, which self-interact through a potential $V(\phi_j)$ and which couple to gravity via a metric of the form

$$ds^2 = -N^2(T, x^i)dT^2 + e^{2\alpha(T,x^i)}(dx^2 + dy^2 + dz^2).$$

The lapse function, N, and the logarithm of the scale factor, $\alpha = \ln a$, are taken to be spatially dependent to describe large scale inhomogeneities. The shift vector N^i has been set to zero and the 3-metric is assumed to be conformally flat. This metric does not describe gravitational radiation, which is dynamically unimportant relative to the scalar field at long wavelengths[23] and decouples from the remaining degrees of freedom at short wavelengths, in linear perturbation theory.[24]

The ADM 3+1 split of Einstein's equations[25] is convenient because all the evolution equations are first order in time derivatives. The dynamical variables are ϕ_j and α and their momenta, $\Pi^{\phi_j} = \dot{\phi}_j/N$ and $H = \dot{\alpha}/N$. Nakao *et al.* [16] also adopted a first order formalism, but here we generalize to self consistently incorporate the metric as well as the scalar fields. We decompose the fields into long wave components, *e.g.*, $\bar{\phi}_j$, and short wave components, *e.g.*, $\delta\phi_j$, which we assume are small: thus, *e.g.*, $\phi_j(T, x^i) = \bar{\phi}_j(T, x^i) + \delta\phi_j(T, x^i)$. In the ADM equations, gradient terms are always multiplied by $e^{-\alpha}$. We neglect all terms which are of second order or higher in spatial gradients, but keep those of first order. For example $\bar{\phi}_{,i}\delta\phi^{,i}$, $\bar{\phi}^{,i}_{,i}$, and ${}^{(3)}R$ are of second order and are dropped. The background equations are the same as those given in SB1 except for stochastic forces describing the short wave communication with the background fields:

$$\bar{H}^2 = \frac{8\pi}{3m_p^2}\Big(\frac{1}{2}\sum_l \bar{\Pi}^{\phi_l 2} + V(\bar{\phi}_j)\Big) \tag{2.1a}$$

$$\bar{H}_{,i} = -\frac{4\pi}{m_p^2}\sum_l \bar{\Pi}^{\phi_l}\bar{\phi}_{l,i} \tag{2.1b}$$

$$\Delta\tilde{\alpha} = \bar{H}\bar{N}\Delta T + \Delta\mathcal{S}_\alpha \tag{2.1c}$$

$$\Delta\bar{H} = \Big\{-\frac{3}{2}\bar{H}^2 + \frac{4\pi}{m_p^2}\Big[V(\bar{\phi}_j) - \frac{1}{2}\sum_l \bar{\Pi}^{\phi_l 2}\Big]\Big\}\bar{N}\Delta T + \Delta\mathcal{S}_H \tag{2.1d}$$

$$\Delta\bar{\phi}_j = \bar{\Pi}^{\phi_j}\bar{N}\Delta T + \Delta\mathcal{S}_{\phi_j} \tag{2.1e}$$

$$\Delta\bar{\Pi}^{\phi_j} = \Big[-3\bar{H}\bar{\Pi}^{\phi_j} - \frac{\partial V}{\partial\bar{\phi}_j}\Big]\bar{N}\Delta T + \Delta\mathcal{S}_{\Pi^{\phi_j}} \tag{2.1f}$$

The first two equations are the energy and momentum constraints. With our choice of metric, the evolution equation for the traceless part of the extrinsic curvature vanishes identically. Since we are considering stochastic processes, we have written the evolution equations in terms of finite

differences, denoted by Δ. The stochastic noise terms, denoted by $\Delta\mathcal{S}$, are due to those short wave fluctuations which have crossed the Hubble radius during the time step ΔT. In the absence of the stochastic terms, these background evolution equations are valid for any choice of time hypersurfaces if second order spatial gradients are neglected. Our choice of time here is governed by the fluctuations that arise within the horizon. In a time step ΔT the scalar fields will undergo a change $\Delta\bar{\phi}_j$ consisting of a classical drift $\bar{\Pi}^{\phi_j}\bar{N}\Delta T$ plus an impulse

$$\Delta\mathcal{S}_{\phi_j} = \sum_{k} \delta\phi_j(T,k)e^{i\mathbf{k}\cdot\mathbf{x}}, \qquad \bar{H}(T)e^{\bar{\alpha}(T)} \leq k < \bar{H}(T+\Delta T)e^{\bar{\alpha}(T+\Delta T)},$$

from all wave modes whose comoving wavenumber k is in the range indicated, *i.e.*, whose wavelengths have exceeded the horizon length during that time step. The impulses for the other variables are a similar sum. The constraint equations do not contain noise terms since there are no explicit time derivatives. The explicit form of $\Delta\mathcal{S}$ will be derived in Sec.B.2.

The stochastic noise terms can be viewed as impulses which continually adjust the initial conditions for the next phase of drift. It is more straightforward to do this for each independent degree of freedom in a first order Hamiltonian formulation than in a second order formulation, where time derivatives of delta-functions would have to be included. This can be seen in the simple example of a one dimensional simple harmonic oscillator obeying $m\ddot{x} + kx = 0$. If we use the coupled first order equations for x and the momentum $p = m\dot{x}$, then the initial conditions, $x(t_0) = x_0$, $\dot{x}(t_0) = p_0/m$ may be incorporated into the equations through delta function source terms: $\dot{x} = p/m + x_0\delta(t-t_0)$, $\dot{p} = -kx + p_0\delta(t-t_0)$. By integrating both of these equations to $t_0 + \epsilon$, we recover the initial conditions provided we take $x(-\infty) = 0 = p(-\infty)$.

To integrate the two constraints equations in (2.1), we follow the analysis in SB1. The momentum constraint implies that the Hubble parameter is a function of the scalar fields and the time parameter, T,

$$\bar{H} \equiv \bar{H}(\bar{\phi}(x^i), T), \quad \text{where} \quad \bar{\Pi}^{\phi_j} = -\frac{m_p^2}{4\pi}\frac{\partial\bar{H}}{\partial\bar{\phi}_j}(\bar{\phi}(x^i), T).$$

Substituting this result into the energy constraint leads to the separated Hamilton-Jacobi equation (SHJE),

$$\bar{H}^2 = \frac{m_p^2}{12\pi}\sum_l \left(\frac{\partial\bar{H}}{\partial\bar{\phi}_l}\right)^2 + \frac{8\pi}{3m_p^2}V(\bar{\phi}_j),$$

a partial differential equation which does not depend explicitly on time. It may be integrated without reference to the evolution equations. We catalogue its solutions by writing $\bar{H} \equiv \bar{H}(\bar{\phi}_j, I_j)$. The n parameters, $I_j \equiv I_j(T)$, $j = 1, n$, are assumed to be spatially independent for simplicity.

One may view this step as a canonical transformation from the independent variables, $\bar{\phi}_j$, $\bar{\Pi}^{\phi_j}$, to new canonical variables I_j, J^j through the relations

$$\Pi^{\phi_j} = -m_p^2/(4\pi)\partial H/\partial\phi_j\,, \qquad J^j = +m_p^2/(4\pi)e^{3\alpha}\partial H/\partial I_j.$$

(The application of canonical transformations to the classical long wavelength problem, including the case where I_j may be spatially dependent, is discussed in Salopek.[23]) In the absence of stochastic forces, the new variables are constant in time.[12] This is not true here. In principle, one could replace the evolution equations in $\phi_j \equiv \phi_j(I_j, J^j)$, $\Pi^{\phi_j} \equiv \Pi^{\phi_j}(I_j, J^j)$ by ones in I_j, J^j, by including diffusion in time. In practice, this proves to be extremely difficult because $n-$parameter solutions of the Hamilton-Jacobi equation are known only for certain classes of

potentials,[23] and, even in these cases, variable changes in stochastic systems must be treated carefully. For example, in going from time T to $T + \Delta T$, the increment ΔI_j must expanded to *second order* in the increments $\Delta\phi_j$ and $\Delta\Pi^{\phi_j}$:

$$\Delta I_j = \frac{\partial I_j}{\partial \phi_k}\Delta\phi_k + \frac{1}{2}\frac{\partial^2 I_j}{\partial\phi_k\partial\phi_l}\Delta\phi_k\Delta\phi_l + \text{other terms in } \Delta\Pi^{\phi^k}, \quad \Delta\Pi^{\phi_k}\Delta\Pi^{\phi_l}, \quad \Delta\phi_k\Delta\Pi^{\phi_l}$$

in order to be accurate to order ΔT since, for example, $\Delta\phi_j$ contains the noise term $\Delta\mathcal{S}_{\phi_j}$ which is of order $\Delta T^{1/2}$ (*e.g.*, see eq.(A5b) in Appendix A).

In this paper, we bypass many of these complications by noting that, in the simplest models, the Hubble function $H(\phi_j, I_j)$ depends rather weakly on I_j so it is unnecessary to accurately monitor the time evolution of I_j. In the absence of stochastic terms, we have already shown[12] that two slightly different solutions of the SHJE approach each other rapidly, with their deviation ΔH behaving as a decaying mode,

$$\Delta\bar{H} \approx \frac{\partial\bar{H}}{\partial I_j}\Delta I_j \propto e^{-3\bar{\alpha}}.$$

In cases where all the fields are moving relatively slowly or where there is an attractor solution for H, it is a good approximation to take I_k as a constant. For example, the slow roll-over approximation, $\bar{H} \approx \bar{H}_{SR}$, where $\bar{H}^2_{SR} = 8\pi V(\bar{\phi}_j)/(3m_p^2)$, contains no arbitrary parameters and the momenta are uniquely determined by $\bar{\Pi}_j = -m_p^2/(4\pi)(\partial\bar{H}_{SR}/\partial\bar{\phi}_j)$. When roll-down is not necessarily slow, it may still be valid to neglect the explicit I_j dependence. An example is a single scalar field moving in an exponential potential for which $\bar{H}$ converges towards an attractor solution, $\bar{H}_{att}$, which differs from $\bar{H}_{SR}$.

Stochastic noise repeatedly perturbs the system away from the attractor, but the system quickly returns to it. Taking the I_j to be constants allows us to drop the evolution equations for H and Π^{ϕ_j}: the number of equations is reduced in half. This is one of the key assumptions in this paper. It greatly facilitates our analysis leading to the exact solutions of Sec. III. There are situations with more than one scalar field, for example with moguls on the potential surface,[8] for which the assumption of constant I_k is probably not valid. In this case, integrating the constraints using Hamilton-Jacobi theory is not very useful, and a different approach is required.[24]

With the neglect of the decaying mode contribution, $\bar{H} \equiv \bar{H}_{att}(\phi_k)$ does not depend explicitly on time. The scalar field momenta are given by partial derivatives of $\bar{H}_{att}$, so the momentum evolution equations, (2.1d,f) may otherwise be disregarded. The system of equations governing the evolution of the inhomogeneous long wavelength background that we solve in this paper are then

$$\bar{H} \equiv \bar{H}(\bar{\phi}_j), \tag{2.2a}$$

$$\bar{H}^2 = \frac{m_p^2}{12\pi}\sum_l\left(\frac{\partial\bar{H}}{\partial\bar{\phi}_l}\right)^2 + \frac{8\pi}{3m_p^2}V(\bar{\phi}_j), \tag{2.2b}$$

$$\Delta\bar{\phi}_j = -\frac{m_p^2}{4\pi}\frac{\partial\bar{H}}{\partial\bar{\phi}_j}\bar{N}\Delta T + \Delta\mathcal{S}_{\phi_j}, \tag{2.2c}$$

$$\Delta\bar{\alpha} = \bar{H}\bar{N}\Delta T + \Delta\mathcal{S}_\alpha. \tag{2.2d}$$

If the time coordinate is chosen to be a function of $\bar{\phi}_j$ and $\bar{\alpha}$, equations (2.2c) and (2.2d) will not be independent. The final number of degrees of freedom is just equal to the number of scalar fields.

We emphasize again that this system is not valid in all situations. The more general case in which one solves equations of the form of (2.1) with the inclusion of noise terms in the momenta requires careful treatment to ensure that the decaying modes are adequately treated numerically, as we describe in Bond and Salopek.[24] Nonetheless (2.2) represents an extremely useful and more accurate generalization of the usual Starobinski slow rollover assumption for stochastic inflation where (2.2a,b) are replaced by $\bar{H} = H_{SR}$, so (2.2c) becomes

$$\Delta\bar{\phi}_j = -\frac{m_p^2}{4\pi}\frac{\partial \bar{H}_{SR}}{\partial\bar{\phi}_j}\Delta t + \Delta\mathcal{S}_{\phi_j}, \qquad \text{where } \frac{\partial\bar{H}_{SR}}{\partial\bar{\phi}_j} = -\frac{1}{3\bar{H}}\frac{\partial V}{\partial\bar{\phi}_j}.$$

In the Starobinski case, the time t is chosen to be synchronous time, with $\bar{N} = 1$. We believe that a more suitable choice of time hypersurface is one on which the comoving Hubble function aH is uniform, as we now justify.

B. Perturbations within the Horizon and The Choice of Time Hypersurface

1. Perturbations on a Homogeneous Background

Before turning to the description of perturbations $\delta\phi_j(T, x^i)$ on an inhomogeneous long wavelength background $\bar{\phi}_j(T, x^i)$ in Sec. B2, we illustrate the main issues on a homogeneous background $\bar{\phi}_j(T)$, using the well developed linear perturbation theory of the metric and scalar fields in the longitudinal gauge, as described in SBB.[8] In the longitudinal gauge, the metric is of the form used in Sec. II.A. To conform to the SBB notation, we let $\Phi_H \equiv \alpha(t, x^i) - \bar{\alpha}(t)$, where $\bar{\alpha}(t)$ is uniform background value, $\bar{N} = 1$ and $\delta N = \Phi_A(t, x^i)$. Thus, we have

$$\phi_j(t, x^i) = \bar{\phi}_j(t) + \delta\phi_j(t, x^i),$$
$$g_{00}(t, x^i) = -(1 + 2\Phi_A(t, x^i)), \quad g_{ij}(t, x^j) = a^2(t)\delta_{ij}(1 + 2\Phi_H(t, x^i)).$$

In linear perturbation theory, the anisotropic stress for scalar perturbations vanishes, which imposes the condition $\Phi_A = -\Phi_H$. As well, in linear theory the scalar field is decoupled from gravitational radiation. The perturbation equations are

$$\left(\frac{m_p^2}{4\pi}\frac{k^2}{a^2} - \dot{\bar{\phi}}_j^2\right)\Phi_H = \dot{\bar{\phi}}_j\delta\dot{\phi}_j + (3\bar{H}\dot{\bar{\phi}}_j + \frac{\partial V}{\partial\bar{\phi}_j})\delta\phi_j, \tag{2.3a}$$

$$\delta H = \dot{\Phi}_H + \bar{H}\Phi_H = -\frac{4\pi}{m_p^2}\dot{\bar{\phi}}_j\delta\phi_j, \tag{2.3b}$$

$$\delta\ddot{\phi}_j + 3\bar{H}\delta\dot{\phi}_j + \frac{k^2}{a^2}\delta\phi_j + \sum_i \frac{\partial^2 V}{\partial\bar{\phi}_j\partial\bar{\phi}_i}\,\delta\phi_i - 2\Phi_H\frac{\partial V}{\partial\bar{\phi}_j} + 4\dot{\bar{\phi}}_j\dot{\Phi}_H = 0. \tag{2.3c}$$

Note that the perturbation to the Hubble function is δH is given by (2.3b), which is the linear perturbation theory version of the momentum constraint equation. Eqs.(2.3a) is the linear perturbation theory version of the energy constraint equation. Of course, eq.(2.3c) is the evolution equation for the scalar field. The equations have been expanded in spatial eigenmodes, which, for the flat universes considered here, are just plane waves $\exp[ik_jx^j]$ labelled by the the comoving wavenumber $\vec{k}$. Substitution of (2.3a,b) into (2.3c) yields an equation solely in $\delta\phi_j$.

For large $k/(Ha)$, the metric terms involving Φ_H and the effective mass matrix $\partial^2 V/\partial\bar{\phi}_j\bar{\phi}_i$ are subdominant, and, to leading order in k/a, we have

$$\delta\ddot{\phi}_j + 3\bar{H}\delta\dot{\phi}_j + \frac{k^2}{a^2}\delta\phi_j = 0. \tag{2.4}$$

This can be solved using the WKB approximation. It admits a positive energy solution describing a ground state wave-function,

$$\delta\phi_j = e^{-ik\int dt/a}/(\sqrt{2k}a), \quad \text{valid for} \qquad k/a > H, \quad (\partial^2 V/\partial\phi_j^2)^{1/2}. \tag{2.5}$$

At horizon crossing, $k/(Ha) = 1$, this solution predicts that the fluctuations leave the horizon with an *rms* amplitude given by the Hawking temperature:

$$[k^3/(2\pi^2)|\delta\phi(k)|^2]^{1/2} = H/(2\pi). \tag{2.6}$$

Of course the WKB approximation breaks down before the time when $Ha = k$. Nonetheless, (2.6) does provide a reasonably accurate result for the horizon crossing amplitude, as determined by the numerical studies of SBB. Further, there is a period after horizon crossing when $\delta\phi_j$ remains approximately constant, before the influence of the metric perturbations causes it to grow. We can illustrate this behavior using the well known exact solution of (2.4) for the case of de Sitter space with H constant, describing the Bunch-Davies vacuum:[26]

$$\delta\phi(t,k) = \frac{H}{\sqrt{2k^3}}\left(i + \frac{k}{Ha}\right)\exp[ik/(Ha)]. \tag{2.7}$$

This agrees with the positive energy solution (2.5) in the large $k/(Ha)$ limit, and in the opposite limit, $k/(Ha) \to 0$, the asymptotic dependence (2.6) is exact. However, in the more general situations where the Hubble parameter varies in time, small deviations of the *rms* fluctuations from the Hawking temperature at Horizon crossing will occur.

One cannot effectively address the issue of time coordinate choice in stochastic inflation without relating it to the short wavelength inhomogeneities, for time is not just some arbitrary integration parameter, but specifies the hypersurface upon which the fluctuations are measured. This issue has largely been ignored in the previous literature. For example, the time used in Starobinski's Fokker-Planck equation (1.2) which is valid in de Sitter space was basically a synchronous time coordinate. Nonetheless, Starobinski did suggest, though without strong justification, that α would be a better choice. If one considers only long wavelength fields without stochastic forces, then we have argued that α is indeed a natural choice of time parameter.[12,23] However, the situation is somewhat altered when one includes the short scale effects as well. This is not yet evident in the longitudinal gauge linear perturbation treatment that led to (2.4) describing quantum fluctuations within the horizon. In longitudinal time, the metric fluctuation $\Phi_H = \alpha(t,x^i) - \bar{\alpha}(t)$ is approximately zero. If α is chosen as time, then, of course, $\Phi_H = 0$ is identically zero. However, because of our crude approximations, this choice of time surface is not completely satisfactory. As we show in the next subsection, the short scale evolution appears simplest on the long wavelength hypersurfaces of constant He^{α}. However, in many cases of interest, H varies slowly compared to e^{α}, so the evolution of the fields as measured on constant α surfaces does not differ greatly form the evolution measured on constant He^{α} surfaces.

2. Perturbations on a Inhomogeneous Background

Even in an inhomogeneous background, we can solve for the short wave fluctuations by introducing a conformal time field, $\tau(T,x^i)$, defined in terms of the background fields by $\dot{\tau}/\bar{N} =$

$e^{-\bar{\alpha}}$. If we choose τ as the time parameter, then the lapse function is $\bar{N} = e^{\bar{\alpha}}$, so the background 4-metric takes the conformally flat form

$$d\bar{s}^2 = e^{2\bar{\alpha}(\tau,x^i)}(-d\tau^2 + dx^2 + dy^2 + dz^2). \tag{2.8}$$

We may relate τ to the physical variables α and ϕ through

$$\tau = \int_{-\infty}^{\bar{\alpha}} d\tilde{\alpha} e^{-\tilde{\alpha}} \bar{H}^{-1} = -1/(e^{\bar{\alpha}}\bar{H}) - \int_{-\infty}^{\bar{\alpha}} d\tilde{\alpha} e^{-\tilde{\alpha}} \bar{H}^{-2}(d\bar{H}/d\tilde{\alpha}). \tag{2.9}$$

For slow rollover of fields, the second term is small so $\tau \approx -1/(\bar{H}e^{\bar{\alpha}})$. Higher order corrections may be found by repeated integration by parts. One could also add an arbitrary function of the spatial coordinates to (2.9), but then τ would not be a function only of the physical fields. Using conformal time as the time parameter is somewhat awkward in that it depends in general upon the past history of the background fields. Instead we adopt

$$T = \ln(\bar{H}e^{\bar{\alpha}}), \tag{2.10}$$

the natural logarithm of the 'comoving wavenumber' at horizon crossing, $k_H = (Ha)$, as the time parameter. An advantage of τ over T is that it is always monotonically increasing as any good time variable should be. During inflation, T is always increasing. However, during the radiation- and matter-dominated regimes, it decreases; but then the stochastic formalism is no longer valid because long wavelength waves cross the horizon to feed the short wavelength fields.

We now show that τ is a logical choice for the time coordinate by solving for scalar field quantum fluctuations on the long wavelength background. Motivated by the result of Sec. B1 that, in the homogeneous background case, the metric back-reaction to scalar field perturbations within the horizon is small, we assume short wavelength metric perturbations are negligible for the long wavelength background, eq.(2.8). It is convenient to introduce new fields $\chi_j(t,x^i) = e^{\bar{\alpha}(t,x^i)}\phi_j(t,x^i)$, which we split into long and short wavelength contributions, $\chi = \bar{\chi} + \delta\chi$. The short wavelength perturbation $\delta\chi$ satisfies

$$-\delta\chi_{j,\mu}{}^{,\mu} + e^{-\bar{\alpha}}[e^{\bar{\alpha}}]_{,\mu}{}^{,\mu}\delta\chi_j + e^{2\bar{\alpha}}\frac{\partial^2 V}{\partial\bar{\phi}_j^2}\delta\chi_l = 0. \tag{2.11}$$

All raised indices are defined using $\eta^{\mu\nu}$. The background equations imply that $e^{-\bar{\alpha}}[e^{\bar{\alpha}}]_{,\mu}{}^{,\mu} = e^{2\bar{\alpha}}[-2\bar{H}^2(\bar{\phi}_j) + (m_p^2/(4\pi))\sum_l(\partial\bar{H}/\partial\bar{\phi}_l)^2]$, where we have neglected second order spatial gradients in the background fields. The final perturbation equation governing $\delta\chi_j$ is then

$$\frac{\partial^2\delta\chi_j}{\partial\tau^2} - \nabla^2\delta\chi_j + e^{2\bar{\alpha}(\tau,x^i)}\Big[-2\bar{H}^2 + \frac{m_p^2}{4\pi}\sum_l\Big(\frac{\partial\bar{H}}{\partial\bar{\phi}_l}\Big)^2 + \frac{\partial^2 V}{\partial\bar{\phi}_j^2}\Big]\delta\chi_j = 0. \tag{2.12}$$

The Fourier transform of this equation is complicated because $e^{2\bar{\alpha}(\tau,x^i)}$ is spatially dependent. However, if the wavelength is much larger than the horizon size, then a Fourier wave solution is a good approximation:

$$\delta\chi_j(\tau,x^i) = e^{i\mathbf{k}\cdot\mathbf{x}}e^{ik\tau}/\sqrt{2k}, \quad \text{if} \quad k^2 > e^{2\bar{\alpha}}\Big|-2\bar{H}^2 + \frac{m_p^2}{4\pi}\sum_l\Big(\frac{\partial\bar{H}}{\partial\bar{\phi}_l}\Big)^2 + \frac{\partial^2 V}{\partial\bar{\phi}_j^2}\Big|.$$

This generalizes the WKB solution (2.5) for a homogeneous background. The normalization of the mode functions is determined by quantum commutation relations (see SBB). At $k\tau \approx 1$, we have

$$\langle \frac{k^3}{2\pi^2} |e^{-\bar{\alpha}} \delta\chi_j|^2 \rangle^{1/2} \approx \frac{\bar{H}}{2\pi},$$

as in the homogeneous case. However, the Fourier solution breaks down around $k\tau \sim 1$, at which time it provides a stochastic impulse to the inhomogeneous background. Evolution will, in general, nonlinearly couple the added waves.

We now derive the noise terms $\delta\mathcal{S}_{\phi_j}$. (From now on, we work with $T = \bar{\alpha} + \ln \bar{H}$ rather than conformal time.) In going from time T to $T + \Delta T$, those wavenumbers which satisfy $e^T \leq |\mathbf{k}| < e^{T+\Delta T}$ are assumed to contribute an impulse to the background scalar field, making the change from

$$\bar{\phi}_j(T, x^i) \text{ to } \bar{\phi}(T, x^i) + \bar{H}\left[\bar{\phi}(T, x^i)\right] \sum_{e^T \leq |\mathbf{k}| < e^{T+\Delta T}} \frac{e^{i\mathbf{k}\cdot\mathbf{x}}}{\sqrt{2k^3}} a_j(\mathbf{k}), \tag{2.14}$$

where we use the notation

$$\sum_{\mathbf{k}} \equiv \int \frac{d^3\mathbf{k}}{(2\pi)^3}.$$

In (2.14), we have used the horizon crossing expression $e^{-\bar{\alpha}(T,x^i)} = \bar{H}(\bar{\phi}_j(T, x^i))/k$. Here, $a_j(\mathbf{k})$ is a complex Gaussian random field, with

$$a_j^*(\mathbf{k}) = a_j(-\mathbf{k}) \quad \text{and} < a_j(\mathbf{k}) a_{j'}(\mathbf{k}') >= (2\pi)^3 \delta^3(\mathbf{k} + \mathbf{k}') \delta_{jj'}.$$

Hence, the stochastic noise term in the long wavelength background equation (2.2c) is

$$\Delta\mathcal{S}_{\phi_j} = \bar{H}\left[\bar{\phi}(T, x^i)\right] \sum_{e^T \leq |\mathbf{k}| < e^{T+\Delta T}} \frac{e^{i\mathbf{k}\cdot\mathbf{x}}}{\sqrt{2k^3}} a_j(\mathbf{k}).$$

It is therefore Gaussian-distributed with zero mean and variance:

$$< \Delta\mathcal{S}_{\phi_m}(T, x^i)\, \Delta\mathcal{S}_{\phi_{m'}}(T', x'^i) >= \delta_{mm'} \frac{\bar{H}(\bar{\phi}_j(x^i))}{2\pi} \frac{\bar{H}(\bar{\phi}_j(x'^i))}{2\pi} \frac{\sin[e^T|\mathbf{x} - \mathbf{x}'|]}{[e^T|\mathbf{x} - \mathbf{x}'|]} \delta_{TT'} \Delta T. \tag{2.15}$$

The amplitude of the stochastic impulse therefore depends upon the local value of the Hawking temperature $H/(2\pi)$. However, it is unclear whether we should take it to be the Hawking temperature evaluated at the beginning of the interval T to $T + \Delta T$, or whether it should be averaged over the interval. As we shall see, this ambiguity leads to different possible operator orderings occurring in the Fokker-Planck equation derived from the stochastic equations. (We prefer evaluating H at T).

The stochastic impulse for $\bar{\alpha}$, $\Delta\mathcal{S}_\alpha$, is related to $\Delta\mathcal{S}_{\phi_j}$, since $\bar{\alpha}$ is defined in terms of T and $\bar{H}(\bar{\phi})$.

The basic assumption behind stochastic inflation and the derivation of the noise term is that one can employ classical random fields to imitate the effects of the quantum fields. If the background were truly homogeneous, we could write the noise term as a quantum field,

$$\Delta\hat{\mathcal{S}}_{\phi_m}(T, x^i) = \sum_{e^T \leq \mathbf{k} < e^{T+\Delta T}} \frac{1}{\sqrt{2k} e^{\bar{\alpha}(T,x^i)}} \left[\hat{a}_m(\mathbf{k}) e^{i(\mathbf{k}\cdot\mathbf{x} + ke^{-T})} + \hat{a}_m^\dagger(\mathbf{k}) e^{-i(\mathbf{k}\cdot\mathbf{x} + ke^{-T})}\right], \tag{2.16}$$

in terms of quantum annihilation and creation operators, $\hat{a}_m(\mathbf{k})$ and $\hat{a}_m^\dagger(\mathbf{k})$, which satisfy the commutation relations, $[\hat{a}_m(\mathbf{k}), \hat{a}_{m'}(\mathbf{k}')] = \delta_{mm'}\,(2\pi)^3\delta^3(\mathbf{k}-\mathbf{k}')$ (see, *e.g.*, SBB). The variance for this quantum field obeys (2.15). However, there is no consistent quantum theory of long wavelength evolution including gravitational effects, and no justification for a quantum noise term like this acting on a quantum long wavelength field. There are heuristic arguments that suggest long wavelength fields behave classically for the most part.[12] Following Starobinski, we model the long wavelength background as the classical Gaussian random field (2.14) with the same dispersion as (2.16). This is an assumption seems reasonable but is extremely difficult to justify. We also re-emphasize that (2.13) is an approximate expression because there will always be some imprecision in the matching between long and short wavelength fields at the Hubble radius.

C. Langevin and Fokker-Planck Equations

With $T = \ln(Ha)$ as time, the lapse is

$$\bar{N}^{-1} = \dot{T}/\dot{N} = \bar{H} - \frac{m_P^2}{4\pi}\frac{1}{\bar{H}}\sum_m \left(\frac{\partial \bar{H}}{\partial \bar{\phi}_m}\right)^2 , \tag{2.17}$$

so the Langevin equation for the scalar field takes the form

$$\Delta\phi_j = -f_j(\phi_m)\Delta T + \Delta\mathcal{S}_{\phi_m}, \tag{2.18}$$

where the classical drift 'force' is

$$f_j(\phi_m) = -\frac{\frac{m_P^2}{4\pi}\bar{H}\,\partial\bar{H}/\partial\bar{\phi}_j}{\left[\bar{H}^2 - \frac{m_P^2}{4\pi}\sum_m \left(\partial\bar{H}/\partial\bar{\phi}_m\right)^2\right]}. \tag{2.19a}$$

and the quantum noise term $\Delta\mathcal{S}_{\phi_m}$ is Gaussian with the expectation value (2.16). (A small diffusion correction to (2.17) ignorable for the applications considered in this paper will be discussed in ref.24.)

In Appendix A, we derive the Fokker-Planck equation for the probability distribution $P(\bar{\phi}_j|T)$ for the field to have values $\bar{\phi}_j$ at a given point x^j at time T from the Langevin equation:

$$\frac{\partial P(\bar{\phi}_j|T)}{\partial T} = -\sum_m \frac{\partial}{\partial\bar{\phi}_m}\left[f_m(\bar{\phi}_j)P(\bar{\phi}_j|T)\right] + \frac{1}{2}\sum_m \frac{\partial^2}{\partial\bar{\phi}_m^2}\left[\left(d(\bar{\phi}_j)\frac{\bar{H}}{2\pi}\right)^2 P(\bar{\phi}_j|T)\right]. \tag{2.19b}$$

The first term on the right describes the classical drift, with force f_m, while the second describes quantum diffusion, whose magnitude is determined by the covariance matrix of the stochastic impulse,

$$< \Delta\mathcal{S}_{\phi_m}(T,x^i)\Delta\mathcal{S}_{\phi_{m'}}(T',x^i) >= \delta_{mm'}\delta_{TT'}\;\Delta T\;\left[d(\bar{\phi}_j)\frac{\bar{H}(\bar{\phi}_j)}{2\pi}\right]^2.$$

A correction factor $d(\bar{\phi}_j)$ has been included because, in the case of rapid evolution, the fluctuations do not leave the horizon at exactly the Hawking temperature. It is usually close to unity, but is difficult to calculate precisely for complicated inflation models. (We touched upon these complications in Sec. B1, but defer a more complete treatment to Bond and Salopek.[24])

The Fokker-Planck equation gives the distribution of scalar field values for a 3-dimensional realization, as well as the probability of finding a field value at a given point. Although this distribution ignores spatial correlations, it is useful for understanding gross features of the full

distribution. For example, one may determine how many points in the 3-D distribution are above a certain threshold, which is often of interest in the theory of structure formation.[27]

The operator ordering in the diffusion term is not unique.[21] This one corresponds to the Ito version of the stochastic equations. We discuss other operator orderings that can arise in Appendix A and when we present exact solutions of eq.(2.19) in Sec. III. In the more general treatment where one does not neglect the decaying mode, the probability function will also depend on the scalar field momentum variables and derivatives with respect to them will also appear on the right hand side. Eq.(2.19b) would then be derived by integrating out the momentum dependence.[24]

The effects of spatial correlations are embodied in the functional Fokker-Planck equation

$$\frac{\partial \mathcal{P}[\phi_j|T]}{\partial T} = \sum_{x^i}\sum_{m}\frac{\delta}{\delta\phi_m(x^i)}\Big[-f_m[\bar{\phi}_j(x^i)]\mathcal{P}[\phi_j|T]\Big]$$
$$+\frac{1}{2}\sum_{x^i,y^i}\sum_{m}\frac{\delta^2}{\delta\phi_m(x^i)\delta\phi_m(y^i)}\Big[\frac{\bar{H}(\bar{\phi}_j(x^i))}{2\pi}\frac{\bar{H}(\bar{\phi}_j(y^i))}{2\pi}\frac{\sin[e^T|\mathbf{x}-\mathbf{y}|]}{[e^T|\mathbf{x}-\mathbf{y}|]}\mathcal{P}[\phi_j|T]\Big]. \qquad (2.20)$$

for the probability functional $\mathcal{P}[\phi_j(x^i)|T]$ describing the distribution of scalar field configurations $\phi_j(x^i)$ on a surface of uniform T. This equation is not of much practical use. If the spatial dependence of the fields is of interest, our preferred approach is direct simulation of a network of Langevin equations to generate 3-D realizations (see Sec. IV).

D. Initial Conditions for Stochastic Inflation

If one wishes to model structure in the Universe, then the initial conditions for the Langevin and Fokker-Planck are relatively straightforward. In the Langevin formalism, one starts with a homogeneous and isotropic comoving lattice with initial background values, ϕ_{j0} and T_0. ($H(\phi_{j0})$ is not an independent free parameter because one typically chooses the attractor solution of the separated Hamilton-Jacobi equation.) In the inflation scenario, all inhomogeneities are assumed to be generated subsequently by quantum noise terms. The starting homogeneous background values are free parameters to be fixed by observations. For example, in the case of a single scalar field, if one chooses the comoving size of the lattice, $2\pi\epsilon^{-T_0}$, to coincide with our observable Universe, one must choose ϕ_0 such that the initial Hubble parameter, $H(\phi_0)/m_{\mathcal{P}} \lesssim 10^{-5}$, in order for the variance of the probability function, $\langle(\Delta\phi)^2\rangle$, to be consistent with microwave background limits (see Sec. III.B.1). One may feel that our choice of initial conditions ignores those physical processes that occurred before our calculations began. However, only inhomogeneities with wavelengths larger than the patch size were produced before the starting time T_0, and their effects, including most nonlinear interactions, may be modelled by employing homogeneous initial values for the scalar fields drawn from distributions (that could be non-Gaussian from the earlier evolution).

The corresponding probability function, $P(\phi_j|T;T_0,\phi_{j0})$, which describes the distribution of scalar field points on the lattice, will be referred to as the Green's function. It thus begins as a delta function distribution, $\lim_{T\to T_0^+} P(\phi_j|T;T_0,\phi_{j0}) = \delta^n(\phi_j-\phi_{j0})$. These initial conditions can be incorporated into the FP equation (2.19b) by adding the delta function term $\delta^n(\phi_j-\phi_{j0})\delta(T-T_0)$ to the right-hand side.

Green's functions at different times, $T_0 < T' < T$, are related through the integral identity

$$P(\phi_j|T;T_0,\phi_{j0}) = \int_{-\infty}^{\infty} d\phi'_j P(\phi_j|T;T',\phi'_j)\,P(\phi'_j|T';T_0,\phi_{j0}) \qquad (2.21)$$

which has a simple physical interpretation. At the intermediate time, T', the initial patch which originated at $T = T_0$ has subdivided into a collection of horizon size cells of comoving wavelength $2\pi e^{-T'}$, where the probability of observing ϕ_0' in one cell is $P(\phi_j'|T'; T_0, \phi_{j0})$. Each of these new cells evolves independently of the others, and at a later time T each has subdivided into smaller horizon size cells of comoving radius $2\pi e^{-T}$ where the probability of observing ϕ is $P(\phi|T; T', \phi')$. The total probability $P(\phi|T; T_0, \phi_0)$ is just the sum over all independent probabilities, eq.(2.21).

The Green's function carries useful information about different length scales through its dependence on ϕ_0. In Sec. F, we show to derive the fluctuation spectrum from the moments of the Green's function. In fact, if non-Gaussian fluctuations are important for galaxy formation, then the Green's function should prove to be a valuable statistic.

E. Asymptotic Behaviour for Stochastic Inflation

At late times, $T - T_0 \to \infty$, the Fokker-Planck solution describes the local distribution of primordial fluctuations which evolve to form the observed cosmic structures. However, to compare our results with cosmological observations, we need to transform from $T = \ln(Ha)$ to other time hypersurfaces. Once quantum diffusion is no longer important, the evolution is simplest if one chooses uniform Hubble surfaces. Indeed $\ln(Ha)$ breaks down as a viable time variable during the transition from inflation to the radiation-dominated era because it is not monotonic. At an even later time, when the length scales of the fluctuations re-enter the Hubble radius, other comoving surfaces are more natural for evolving the multi-component fluid system of radiation and matter. The synchronous and longitudinal gauges are the usual choices within the context of linear perturbation theory. Metric fluctuations in the longitudinal gauge are especially useful because they generalize the Newtonian potential.

Since the variance of the quantum diffusion term in eq.(2.18) is proportional to H^2, it diminishes as the probability function moves down the potential and becomes unimportant when $H^2/(4\pi^2)$ is smaller than $< (\Delta\phi)^2 >$, as determined from the distribution (given homogeneous starting conditions for the patch of the universe we are interested in). Beyond that time, the Universe may still inflate, but the evolution of $P(\phi|T)$ is governed totally by the classical drift:

$$\frac{\partial P(\phi_m|T)}{\partial T} = -\frac{\partial}{\partial \phi_j}[f_j(\phi_m)P(\phi_m|T)]. \tag{2.22}$$

In the case of a single scalar field moving in an arbitrary potential, one can solve the asymptotic equation by choosing ϕ as time. Let $P(T|\phi)$ denote the probability of observing the field T on a uniform ϕ surface. Provided quantum diffusion has ended, it is related to $P(\phi|T)$ through a hypersurface transformation (see SB1, Sec.IV.D):

$$P(T|\phi) = f(\phi)P(\phi|T), \tag{2.23}$$

where $f(\phi)$ is given by (2.19a). The resulting equation,

$$\frac{\partial P(T|\phi)}{\partial \phi} + \frac{1}{f(\phi)}\frac{\partial P(T|\phi)}{\partial T} = 0 \tag{2.24}$$

has wave-like solutions

$$P(T|\phi) = g(T - T_0 - t(\phi)), \quad \text{where} \quad t(\phi) = \int_{\phi_0}^{\phi} \frac{d\phi'}{f(\phi')} \tag{2.25}$$

and g is an arbitrary function. The distribution which uses ϕ as time has the advantage that all the moments $< (\Delta_\phi T)^n >$ for $n \geq 1$ are constant. This property is a reflection of the fact that the variable $\zeta \equiv 3\Delta_\phi \alpha = 3\Delta_\phi T$ is constant in time — with Δ_ϕ denoting a difference on a uniform ϕ surface. (This definition of ζ given in SB1 extends to general nonlinear fields the usual linear perturbation theory ζ introduced by Bardeen, Steinhardt, and Turner.[28]) Thus once the diffusion has ended, it is natural to choose ϕ rather than T for time. Actually H is a better choice, since ϕ is not monotonic at the end of inflation when it starts oscillating. H is a function of ϕ only during inflation and yet is monotonic during the subsequent evolution.

F. A Fluctuation Measure as a Function of Physical Volume

There are practical limits to what can be computed in stochastic inflation. The obvious approach is to simulate the Langevin equation network for a lattice, but it is currently impractical to expect we can go much beyond 128^3 or, possibly, 256^3 points. This would apparently limit the range of T that could be followed for any one given realization to at most 5. One possible way to avoid this is to nest the lattices, starting from very large scale ones, then progressively decreasing the size as T increases. This would be a major computational undertaking.

What we wish to have is a measure of the amplitude of the fluctuations which is easy to compute. Here, we advocate the *rms* fluctuation level α on uniform ϕ surfaces as a function of the initial condition ϕ_0 as such a measure. This turns out to be a measure of how ζ fluctuations change with varying lattice sizes. Yet this function can be determined from solutions of the one point Fokker-Planck equation alone as we now show.

Although one may have expected that all knowledge about spatial correlations is lost in the single-point probability function (2.25), since the initial condition parameter ϕ_0 is correlated with the volume of the lattice, one may recover much useful information about spatial averages on different volume scales.

If N_L is the number of points in a fixed comoving lattice, then $N_L P(T|\phi)dT$ gives the number of cells in the lattice with field values between T and $T + \Delta T$ for a given value of ϕ. The comoving length of the lattice on the side would be $(2\pi)e^{-T_0}$, hence each lattice cell is associated with the same fixed comoving volume $U = (2\pi)^3 e^{-3T_0}/N_L$. The physical volume each cell has stretched to as measured on a uniform ϕ surface is

$$v_{\rm cell} = a^3(T)U = N_L^{-1} e^{3(T-T_0)} \Big(\frac{H(\phi)}{2\pi}\Big)^{-3} = N_L^{-1} e^{3(\alpha-\alpha_0)} \Big(\frac{H(\phi_0)}{2\pi}\Big)^{-3}.$$

The distribution of these physical cell volumes is

$$P(v_{\rm cell}|\phi;\phi_0)dv_{\rm cell} = \frac{1}{3v_{\rm cell}} P(T|\phi;\phi_0)dv_{\rm cell}. \tag{2.26}$$

The lattice, on average, will encompass a physical volume

$$V(\phi|\phi_0) = N_L\langle v_{\rm cell}|\phi;\phi_0\rangle = \int a^3 N_L U\, P(T|\phi;\phi_0)\, dT. \tag{2.27a}$$

Since the hypersurface transformation from T to ϕ is valid only after quantum diffusion has ended, we must use the asymptotic expression (2.25) to evaluate (2.27a). This yields

$$V(\phi|\phi_0) = e^{3t(\phi)} \Big(\frac{H(\phi)}{2\pi}\Big)^{-3} \int_{-\infty}^{\infty} du e^{3u} g(u), \tag{2.27b}$$

where we changed from T to $u = T - T_0 - t(\phi)$. This expression is independent of T_0, and the time parameter ϕ is contained solely in the prefactor before the integral. As a result of continued quantum diffusion, however, the integral (2.27a) may actually diverge. This can be traced to the problem of eternal inflation. The integrals must be regulated to ensure convergence. This is done by integrating only over that region in which quantum diffusion is unimportant, as we show for our exact solutions in Sec. III. For regions that are not eternally inflating, there is a one to one correspondence between the physical volume of the lattice and the initial homogeneous value of the scalar field.

One can also calculate the various moments of the distribution function (2.25) using the volume weight factor (2.27a)

$$< (\Delta T)^n | \phi; \phi_0 >_{V_\phi} \equiv \frac{1}{V(\phi|\phi_0)} \int_{-\infty}^{\infty} dT\, (T - T_0)^n e^{3(T-T_0)} \Big(\frac{H(\phi)}{2\pi}\Big)^{-3}\, g(T - T_0 - t(\phi)). \quad (2.28)$$

The subscript V_ϕ is a reminder that the moments are calculated as a volume average on a uniform ϕ surface. Of primary interest is the second moment, $< (\Delta T)^2 | \phi; \phi_0 >_{V_\phi}$, which gives the variance of T fluctuations. Once again, it is independent of T_0; it depends only on ϕ and ϕ_0. If one eliminates ϕ_0 in favor of the volume of the lattice (2.27), one may interpret this quantity as the fluctuations that are expected in a volume V. In linear theory, the power spectrum for ζ would be defined as the variance of 3α per $\ln(k)$ interval,[8] where k is the comoving wavenumber, on uniform Hubble (or constant ϕ surfaces). It is therefore the derivative of the variance $\langle (\Delta T)^2 | \phi; \phi_0 \rangle$ with respect to $\ln V_{co}^{\frac{1}{3}}$, where the comoving volume $V_{co} \propto k^{-3}$. We now define the nonlinear fluctuation function in terms of a derivative per *physical volume*:

$$\mathcal{F}(\phi, V) \equiv 3 \frac{d < (\Delta T)^2 >_{V_\phi}}{d \ln V} = 3 \frac{d < (\Delta T)^2 (\phi, \phi_0) >}{d\phi_0} \Big(\frac{\partial \ln V(\phi|\phi_0)}{\partial \phi_0}\Big)^{-1}. \quad (2.29)$$

If the fluctuations $< (\Delta T)^2 (\phi_0) >$ are small, this reduces to the fluctuation spectrum of linear perturbation theory as defined by SBB. A non-Gaussian example of its utility is given in Sec. III.

G. Reheating and Connection with Observables

Our analysis holds as long as the Universe is scalar field dominated. However, at some time the scalar field energy is transformed into radiation and matter. For wavelengths longer than the Hubble radius, fluctuations do not evolve during the radiation and matter-dominated eras. For example, the fluctuation function defined by (2.29) remains invariant. For our purposes here, the longitudinal gauge is convenient for evolving fluctuations after the heating of the Universe, both outside and inside the Hubble radius, for the metric fluctuation $\Delta_L \alpha = \Phi_H$ is a natural relativistic generalization of the Newtonian potential. For matter-dominated flat universes (and adiabatic perturbations), large angle microwave background fluctuations provide a direct measure of Φ_H, through the Sachs-Wolfe effect.

Within the horizon, one must then solve the perturbation equations for a multi-component fluid of radiation and matter.[29] During the radiation-dominated phase, perturbations oscillate within the Hubble radius because of pressure and damp as a result of the Hubble expansion. However, during the matter-dominated phase, Φ_H is constant both outside and within the Hubble radius. According to Sec. II of SBB, during the matter dominated era, $\Delta_L \alpha$ is related to $\Delta_H \alpha$ by

$$\Phi_H \equiv \Delta_L \alpha = \frac{3}{5} \Delta_H \alpha. \quad (2.30)$$

The Sachs-Wolfe relation for microwave background temperature anisotropies $\Delta T_{cmb}/T_{cmb}$ (valid for large angles, $\theta \gtrsim 3^0$) is

$$\Delta T_{cmb}/T_{cmb} = -\Phi_H/3 = -\Delta_H a/5 = -\Delta_H \ln(Ha)/5, \tag{2.31}$$

where $\Delta_H \ln(Ha)$ is the deviation in $\ln(Ha)$ on a uniform Hubble surface. (Because the symbol T has already been used to label our time coordinate, we will use T_{cmb} to denote the microwave background temperature.) To give a precise comparison with microwave background observations, maps of microwave background anisotropies could be computed by doing a stochastic inflation simulation for a lattice which forms a spherical shell corresponding to the surface of last scattering. One would have to include such details as a last scattering surface of finite thickness, transfer function modifications of Φ_H describing the differences in fluctuation evolution from the radiation-dominated to the matter-dominated phases and Thompson scattering by ionized gas at photon decoupling. Then, to compare with a given experiment, the map would have to be convolved with the experimental beam profile. In this paper, we are only interested in rough estimates of how current microwave background limits constrain stochastic inflation models, and can ignore most of these effects. If instrumental effects (beam smearing *etc.*) are neglected, temperature anisotropies can be estimated directly from (2.31). In that case, the probability function (2.25) would give the distribution of anisotropies in a two dimensional slice, provided we adopted initial conditions to make the scalar field fluctuations in the current Hubble volume initially homogeneous. We emphasize however that a careful treatment is required to accurately compute the anisotropies expected for realistic experimental configurations and refer the reader to Bond[30] and Bond and Salopek[24] for further discussion.

III. FOKKER-PLANCK GREEN'S FUNCTION SOLUTIONS FOR AN EXPONENTIAL POTENTIAL

An extremely useful model for providing concrete analytic illustrations of general principles in inflation cosmology is a single scalar field driven by an exponential potential

$$V(\phi) = V(0)\exp\Big[-\sqrt{\frac{16\pi}{p}}\frac{\phi}{m_p}\Big] \ . \tag{3.1}$$

Lucchin and Matarrese[31] were the first to give exact solutions of the cosmological background equations for this system. We extended their work by finding general integrals, including transients, of the separated Hamilton-Jacobi equation, and by analytically evolving the long wavelength background fields.[12,23] We have also found exact solutions of the Wheeler-deWitt equation for homogeneous quantum fields.[12] Sahni[32] found elegant exact solutions for a massless scalar field on a cosmological background generated by such a potential. Ratra[33] obtained exact solutions of the cosmological perturbation equations in synchronous gauge.

The Fokker-Planck equation for an exponential potential was first investigated by Ortolan, Lucchin, and Matarrese,[20,21] who applied both approximate analytic methods and numerical techniques within Starobinski's formalism for stochastic inflation. Here, we derive analytic Green's function solutions of our Fokker-Planck equation for an exponential potential, which incorporates the metric back-reaction by utilizing Hamilton-Jacobi theory and uses our natural choice for the time coordinate. In this section, we drop the bar notation that labelled long wavelength fields: $\bar{\phi}$ is now just ϕ. We also denote $P(\phi|T)$ by $P_T(\phi)$ and $P(T|\phi)$ by $P_\phi(T)$.

A. Derivation of Analytic Green's Functions

To obtain the Green's function for the Fokker-Planck (FP) equation of Sec. II.D one must first find the attractor Hubble function solution of the SHJE to insert into the diffusion and drift terms of the FP equation. The attractor solution,

$$H_{att}(\phi) = H(0)\exp\Big(-\sqrt{\frac{4\pi}{p}}\phi/m_{\mathcal{P}}\Big), \quad H(0) = \Big[\frac{8\pi V(0)}{3m_{\mathcal{P}}^2(1-\frac{1}{3p})}\Big]^{1/2}, \tag{3.2}$$

of the SHJE, eq.(2.2b), for a single scalar field moving in an exponential potential (3.1), given in SB1, is easily verified by direct substitution. Here, $H(0)$ is the value of Hubble parameter at $\phi = 0$. In the absence of the noise terms, the classical trajectories associated with this Hubble function move with the same constant speed:

$$\phi_{cl}(T) - \phi_{cl}(0) = \frac{m_{\mathcal{P}}}{\sqrt{4\pi p}}\frac{1}{1-1/p}(T - T_0)\,. \tag{3.3}$$

As we discuss in Appendix A, there are a number of possible choices for the form of the Langevin equation and the form of the quantum diffusion term in the Fokker-Planck equation. We encompass these orderings by writing the diffusion term in the form

$$(\partial/\partial\phi)[H^{2-2\beta}(\partial/\partial\phi)(H^{2\beta}P_T)],$$

where β is a parameter ranging from 0 to 1. It measures whether in evaluating the stochastic noise contribution over the interval ΔT the Hawking temperature chosen is weighted more strongly at the beginning of the interval, T (β=1), at the end $T + dT$ (β=0), or in between (half way, at $T + dT/2$, has $\beta = 1/2$). The two main forms are β=1 and $\beta = 1/2$, with the β=1 case following if the Ito form of the Langevin equation is adopted, and the $\beta = 1/2$ case if the Stratanovich form is adopted. We believe the spirit of stochastic inflation, with fluctuations leaving the Hubble radius with a background Hawking temperature, is most nearly met if the Hawking temperature is chosen at the beginning of the discrete timestep. This corresponds to the Ito formulation with $\beta = 1$ in Sec. II. Here we are more general. The FP equation is

$$\begin{aligned}\frac{\partial P_T}{\partial T} &= -\frac{m_{\mathcal{P}}}{\sqrt{4\pi p}}\frac{1}{1-1/p}\frac{\partial P_T}{\partial\phi} \\ &+ \frac{d^2H^2(0)}{8\pi^2}\frac{\partial}{\partial\phi}\Big\{\exp\Big[-\sqrt{\frac{16\pi}{p}}\frac{\phi}{m_{\mathcal{P}}}(1-\beta)\Big]\frac{\partial}{\partial\phi}\Big[\exp(-\sqrt{\frac{16\pi}{p}}\frac{\phi}{m_{\mathcal{P}}}\beta)P_T\Big]\Big\} \\ &+ \delta(T-T_0)\delta(\phi-\phi_0).\end{aligned} \tag{3.4}$$

The parameter d is determined by precisely what approximations we adopt for treating the short wavelength fluctuations, and is discussed more fully in ref. 24. For slow rollover d is unity. For exponential potentials, it can be taken to be a constant which tends to unity as $p \to \infty$, and deviates slightly from unity for smaller p.

To solve (3.4), we apply variable changes and Laplace transforms to obtain a first order pde solvable by the method of characteristics. The solution is

$$P(\phi|T;\,T_0,\phi_0) \;=\; \sqrt{\frac{16\pi}{pm_{\mathcal{P}}^2}}\,y^{-1}e^{-(1+z^2)/y}\;z^{\beta+1}\,I_{\beta-1}(2z/y). \tag{3.6a}$$

where $I_{\beta-1}$ is the modified Bessel function of order $\beta - 1$. The function $z(\phi, T)$ is

$$z(\phi,T) \;=\; \exp\Big(\sqrt{\frac{4\pi}{p}}\frac{\phi-\phi_0}{m_{\mathcal{P}}} - \frac{T-T_0}{p-1}\Big) \tag{3.6b}$$

and the function $y(T)$ is

$$y(T) = \frac{d^2}{\pi}(1-1/p)\frac{H^2(\phi_0)}{m_p^2}\Big[1-e^{-2(T-T_0)/(p-1)}\Big]. \tag{3.6c}$$

(The coefficient $H(\phi_0)$ should not be confused with the $H(0)$ of (3.6c), which it equals only for $\phi_0 = 0$.)

Before turning to the interpretation and consequences of this analytic solution in Sec. B, we first sketch the derivation of (3.6), which the reader may wish to skip. It is useful to change variables from ϕ, P_T to u, Q, where

$$u = \exp(\sqrt{\frac{16\pi}{p}}\phi/m_p), \qquad P_T = uQ, \quad \text{with} \quad 0 < u < \infty, \tag{3.7}$$

so the FP equation becomes first order in u and second order in $\partial/\partial u$:

$$\frac{\partial Q}{\partial T} = -a\frac{\partial}{\partial u}(uQ) + f\frac{\partial Q}{\partial u} + b\frac{\partial}{\partial u}(u\frac{\partial Q}{\partial u}) + c\,\delta(T-T_0)\,\delta(u-u_0). \tag{3.8a}$$

The constants in this equation are

$$a = 2/(p-1), \quad b = \frac{2d^2}{\pi p}\frac{H^2(0)}{m_p^2}, \quad c = \sqrt{\frac{16\pi}{pm_p^2}}, \quad \text{and} \quad f = (1-\beta)b. \tag{3.8b}$$

Eq.(3.8a) is first order in u and second order in $\partial/\partial u$. A Laplace transform in u space, $\tilde{Q}(T,s) = \int_0^\infty e^{-su}Q(T,u)du$, yields a first order partial differential equation,

$$\frac{\partial \tilde{Q}}{\partial T} = s(f-b)\tilde{Q} + s(a-bs)\frac{\partial \tilde{Q}}{\partial s} \tag{3.9a}$$

obeying the initial condition

$$\tilde{Q}(T_0,s) = ce^{-su_0}. \tag{3.9b}$$

(The Laplace transform is preferable over a Fourier transform since the domain of u is from 0 to ∞.) A further change of variables from $(s, \tilde{Q})$ to (m, R) gives a simple pde

$$\partial R/\partial T + \partial R/\partial m = 0, \quad m \equiv a^{-1}\ln(1-a/(bs)), \quad R \equiv \Big(s(m)-\frac{a}{b}\Big)^{1-f/b}\tilde{Q}, \tag{3.10}$$

whose solution has the form of a wave moving to the right: $R = g(m-T)$ where g is an arbitrary function. In our case, g is determined by the initial conditions eq.(3.9b), yielding

$$\tilde{Q}(T,s) = ce^{-1/y}x^\beta(s+x)^{-\beta}\exp(\frac{xy^{-1}}{s+x}), \tag{3.11}$$

where the function $x(T)$ is defined by

$$x = \frac{\pi m_p^2}{d^2(1-1/p)H^2(0)}\frac{1}{e^{2(T-T_0)/(p-1)}-1},$$

and y is given by (3.6c). Abramowitz and Stegun[34] give the inverse Laplace transform in terms of $I_{\beta-1}$. Back substitution leads to eq.(3.6).

B. Discussion of Exact Solutions

The exact solution (3.6) is rich in structure. To understand it better, we consider various special cases in this subsection: (1) the late time behaviour as $T - T_0 \to \infty$; (2) solutions with $H(\phi_0)/m_{\mathcal{P}} \ll 1$; corresponding to initial conditions for our observable patch of the Universe; (3) solutions with $H(\phi_0)/m_{\mathcal{P}}$ of order unity, which has pronounced non-Gaussian characteristics; and (4) the effects of different factor orderings and boundary conditions in the Fokker-Planck equation.

1. Late Time Evolution of the Probability Function and Observational Consequences

At late times, the diffusion contribution to the probability distribution (3.6c) becomes unimportant, as suggested in Sec. II.E: it is a function of z only, describing a shape invariant wave, since y approaches the constant $d^2\pi^{-1}(1-1/p)H^2(\phi_0)/m_{\mathcal{P}}^2$. To relate to observables, we perform a hypersurface transformation from T to the uniform H surface, which is the uniform ϕ hypersurface for one scalar field. This is trivial because the fluctuations are linearly related through (3.3):

$$\Delta_T\phi = -\frac{m_{\mathcal{P}}}{\sqrt{4\pi p}}\frac{1}{1-1/p}\,\Delta_\phi T\ . \tag{3.12a}$$

Through eq.(2.31), for a given choice of $H(\phi_0)$, this asymptotic probability function is related to large angle Sachs-Wolfe microwave background fluctuations, subject of course to all of the caveats described in Sec. II.G:

$$\Delta T_{cmb}/T_{cmb} = +\sqrt{4\pi p}\,(1-1/p)\left(\Delta\phi(T)/m_{\mathcal{P}}\right)/5\ . \tag{3.12b}$$

The sign of this relation is easily understood. Where $\Delta\phi$ is negative, the ϕ energy density fluctuation is positive, so the gravitational potential $(-\Phi_H)$ is negative, as is the temperature fluctuation.

Recall from Sec. II.F that we can consider the specification of a sequence of initial conditions for the constrained probability as roughly corresponding to the specification of a set of smoothings over various comoving volumes of the fluctuation level. In particular, we can take the initial value of the Hubble parameter $H(\phi_0)$ as this measure. In Fig. 1, we show a numerical calculation of the scalar field dispersion, $<(\Delta\phi)^2>^{1/2}$, as a function of $H(\phi_0)$, for the case $p = 5$. The dispersion grows linearly with $H(\phi_0)$ until $H(\phi_0) \sim m_{\mathcal{P}}$, where it levels off at a constant value because of nonlinear effects. To satisfy current large scale microwave background constraints, the smoothed temperature fluctuations must be below a few times 10^{-5}. Through eq.(3.12b), we find the allowed initial fluctuation level for our patch of the Universe must satisfy $H(\phi_0)/m_{\mathcal{P}} \lesssim 10^{-5}$. To ensure that the patch with this bound would have stretched enough to encompass our current Hubble volume imposes a constraint on when inflation ended, *i.e.*, when reheat occurred: we require $e^{T_0} \gtrsim 10^{-4}\mathrm{Mpc}^{-1}$. Patches which started with $H(\phi_0)/m_{\mathcal{P}} \sim 1$ would, on the other hand, correspond to a length far exceeding our present horizon radius to avoid violating microwave background limits (see Sec. IV.B.2).

2. Probability Function for our Observable Patch of the Universe

Since, from Sec. B.1, the initial fluctuation level for our patch of the Universe must satisfy $H(\phi_0)/m_p \lesssim 10^{-5}$, the argument of the modified Bessel function in (3.6) is very large, and the asymptotic expansion, $I_{\beta-1}(x) \sim e^x/\sqrt{2\pi x}$, can be used:

$$P(\phi|T;T_0,\phi_0) \sim \sqrt{\frac{4}{ypm_p^2}}\, z^{\beta+1/2}\, \exp\Big[-\frac{(z-1)^2}{y}\Big] .$$

Since $y \sim (H(\phi_0)/m_p)^2$ is small, and $z-1 \sim \sqrt{y}$, the exponential in (3.6b) can be expanded: $z-1 \sim (4\pi/p)^{1/2}(\phi-\phi_0)/m_p - (T-T_0)/(p-1)$. Thus, for these small values of $H(\phi_0)/m_p$, the constrained probability is Gaussian to high accuracy:

$$P(\phi|T;T_0,\phi_0) \approx \sqrt{\frac{4}{ypm_p^2}}\, \exp\Big[-\frac{[(T-T_0)/(p-1) - \sqrt{4\pi/p}(\phi-\phi_0)/m_p]^2}{y}\Big] , \qquad (3.13)$$

a result which is independent of β: the factor ordering problem is not important for the observable fluctuations. The exact distributions for this starting $H(\phi_0)/m_p$ for various T, shown in in Fig. 2, explicitly illustrate how close to Gaussians the distributions are.

Our conclusion that the observable fluctuations will be Gaussian-distributed for an exponential potential agrees qualitatively with other workers. Bardeen and Bublik[13] numerically integrated a similar Fokker-Planck equation and found that Gaussian fluctuations would arise in $\lambda\phi^4/4$ theory, a result confirmed by Hodges[22] using an analytical integration of the Langevin equation. We have shown that this conclusion remains valid even if the effects of metric fluctuations are included and if different operator orderings are considered.

In the large $T-T_0$ limit, the mean and dispersion vary according to

$$<\phi> = \phi_0 + \frac{m_p}{\sqrt{4\pi p}}\frac{(T-T_0)}{1-1/p} \quad \text{and} \quad <(\Delta\phi)^2> \equiv w^2 = \frac{d^2(p-1)}{8\pi^2}H^2(\phi_0). \qquad (3.14)$$

As noted in Sec. II.D., when quantum diffusion is no longer important it is particularly useful to use ϕ as time. The probability function, $P(T|\phi)$, on a uniform ϕ surface is given by the hypersurface transformation (2.23),

$$P(T|\phi) = [\pi y(p-1)^2]^{-1/2}\, \exp\Big[-\frac{u^2}{y(p-1)^2}\Big], \quad \text{where} \quad u = T - T_0 - \sqrt{4\pi p}(1-p^{-1})\frac{(\phi-\phi_0)}{m_p} .$$

The first two moments are

$$<T(\phi)> = T_0 + \sqrt{4\pi p}(1-p^{-1})\frac{(\phi-\phi_0)}{m_p}, \quad \text{and} \quad <(\Delta T(\phi))^2> = \frac{d^2(p-1)^3}{2\pi p}\frac{H^2(\phi_0)}{m_p^2}. \qquad (3.15)$$

Thus, the dispersions approach constant values which depend primarily on the initial value of $H(\phi_0)/m_p$.

To calculate the fluctuation spectrum, we need to determine how the the physical volume of the lattice depends on ϕ_0 through eq.(2.27b),

$$V(\phi|\phi_0) = \Big(\frac{H(\phi_0)}{2\pi}\Big)^{-3}\Big[\frac{H(\phi)}{H(\phi_0)}\Big]^{-3p}\exp\Big[\frac{9d^2}{4\pi p}(p-1)^3\frac{H^2(\phi_0)}{m_p^2}\Big] \approx \Big(\frac{H(\phi_0)}{2\pi}\Big)^{-3}\Big[\frac{H(\phi)}{H(\phi_0)}\Big]^{-3p}. \qquad (3.16)$$

The exponential term due to quantum diffusion actually increases the volume over what one would naively expect, but, for $H(\phi_0)/m_{\mathcal{P}} << 1$, it is not significant and may be safely neglected. The variance in T calculated using a volume average, eq.(2.28), turns out to be (3.15) re-expressed in terms of the physical volume rather than ϕ_0:

$$< (\Delta T)^2 >_{V_\star} = \frac{d^2(p-1)^3}{2\pi p} \frac{H^2(\phi_0)}{m_{\mathcal{P}}^2} = \frac{d^2(p-1)^3}{2\pi p} \frac{1}{m_{\mathcal{P}}^2} \left[(2\pi)^{-3} V H^{3p}(\phi)\right]^{\frac{2}{3(p-1)}}. \tag{3.17}$$

According to eq.(2.29), the fluctuation spectrum is given by differentiation with respect to the volume factor:

$$\mathcal{F}(\phi, V) = \frac{d^2(p-1)^2}{\pi p} \frac{\left[(2\pi)^{-3} V H^{3p}(\phi)\right]^{\frac{2}{3(p-1)}}}{m_{\mathcal{P}}^2}. \tag{3.18}$$

If we define a physical 'wavenumber' scale by $k_{phys} \equiv V^{-1/3}$, then we obtain the usual k-dependence,[31,8] $\mathcal{F} \propto k_{phys}^{-2/(p-1)}$, found in linear perturbation theory.

3. Ultra Large Scale Structure of the Universe

If we consider values of the initial Hubble parameter which are large, then the fluctuation distribution at a point will describe contributions from scales which are very much larger than our current Hubble radius and are thus unobservable. In Fig. 3, we plot the final probability distribution for $H(\phi_0) = m_{\mathcal{P}}$. The distribution is non-Gaussian and noticeably skewed. It has a short tail at positive values of $\phi - \phi_{cl}$, and an exponential tail for negative values. The peak in the distribution occurs to the right of the median because of the nonlinear stochastic force. Some points which were initially kicked to the left eventually get strongly kicked to the right. On occasion, this last kick may exceed the sum of all the past kicks because the stochastic force increases exponentially with negative ϕ; hence the peak moves to the right of the mean. However, the exponential tail is the most striking feature of this distribution because it dramatically increases the number of high density peaks. (Contour maps of a large $H(\phi_0)/m_{\mathcal{P}}$ non-Gaussian case and a small $H(\phi_0)/m_{\mathcal{P}}$ Gaussian case are compared in Fig. 7.) This distribution, however, does not correspond to a distance scale which is physically observable. Matarrese, Ortolan, and Lucchin[21] have integrated the Fokker-Planck equation numerically for this same situation. Since we integrate different equations which self-consistently include the metric back-reaction, our results are quantitatively different. Even so, we cannot be confident that all features of these high $H(\phi_0)/m_{\mathcal{P}}$ cases are properly treated, since quantum gravity corrections are important at such large energy densities, so our formalism breaks down.

Starobinski[10] and Goncharov *et al.* [17] described the phenomenon of eternal inflation in which quantum diffusion can overcome the classical drift in the Langevin equation to drive some patches of the Universe to larger and larger values of the Hubble parameter. Although exceedingly rare in comoving volume, these regions would grow exponentially large to dominate the physical volume and might never reheat. Hence, the Universe would inflate 'eternally'.

We also find that eternal inflation is generic. However, with our choice of time hypersurface, it is not immediately evident in our exact solutions. Indeed, the distr bution (3.6) rolls down the potential without demonstrating any irregularity as $\phi \rightarrow -\infty$. However, if one transforms to the ϕ-hypersurfaces then the eternal inflation becomes manifest. If quantum diffusion is no longer important, the probability of observing the field T on a constant ϕ surface, $P(T|\phi)$, is just $P(\phi|T)$ up to a constant of proportionality according to (2.23):

$$P(T|\phi) = \frac{m_{\mathcal{P}}}{\sqrt{4\pi p}} \frac{1}{1-1/p} P(\phi|T). \tag{3.19}$$

(Although it is unclear how to evaluate $P(T|\phi)$ if diffusion is still important, we can use (3.19) to illustrate the basic behavior.) We denote the contribution to the physical volume of the lattice on a uniform ϕ surface $V(\phi|\phi_0)$ introduced in II.F, from fields in the interval $(T, T+\Delta T)$ by $dV(\phi|\phi_0) = a^3 N_L U P(T|\phi;\phi_0)$ (see 6). This function of T is strongly peaked about the classical trajectory (3.3). However, in the large T limit,

$$dV(\phi|\phi_0) \to \Big(\frac{H(\phi_0)}{2\pi}\Big)^{-3} \frac{2}{p-1} y^{-1} e^{-1/y} \exp\Big[(T-T_0)(3-\frac{2}{p-1}+2\sqrt{\frac{4\pi}{p}}\frac{(\phi-\phi_0)}{m_{\mathcal{P}}}\Big],$$

diverges if $p > 4/3$ and $\beta = 1$. Thus, on a uniform ϕ surface, the probability distribution is dominated by points with large T and thus large a.

Eternal inflation is the source of several technical problems. Since the total physical volume diverges, the integrals that define the fluctuation function (2.29) are not well defined, a cause of difficulty even for $H(\phi_0)/m_{\mathcal{P}} \ll 1$. In deriving the fluctuation spectrum (3.13), we conveniently ignored the divergence by applying an asymptotic expansion of the Bessel functions. However, for $H(\phi_0) \sim m_{\mathcal{P}}$, it is not clear where one should truncate the distribution. For this reason, we often use the probability function on a constant T surface to describe the scalar field fluctuations.

4. Factor Ordering Problems and Boundary Effects in the Fokker-Planck Equation

As we noted in Sec. II, for cases of interest for structure formation, different choices of operator ordering do not alter the probability function (3.6) significantly. However, dramatic deviations occur for $H(\phi_0) \sim m_{\mathcal{P}}$. In this subsection, we investigate the consequences of different operator ordering as well as the effect of boundary conditions at $\phi = -\infty$.

The large $T - T_0$ Fokker-Planck distributions for $H(\phi_0)/m_{\mathcal{P}} = 3$ are plotted in Fig. 4 for the orderings associated with $\beta = 0, 1/2$ and 1. These probability functions are noticeably skewed, with long tails at negative values of $\ln(z)$. Note that the distributions have a median which deviates significantly from $\ln(z) = 0$, the value it would have if the initial delta function in ϕ moved only according to the classical drift.

As one can infer from Fig. 4, our exact solutions conserve probability for $\beta > 0$, but not for $\beta = 0$. Since the stochastic force grows exponentially with $-\phi$, some paths may apparently diffuse to $\phi = -\infty$ in a finite time, where they could be either absorbed or reflected (re-emitted), depending upon the boundary conditions. The boundary condition which preserves probability may be found by integrating (3.4) from $\phi = -\infty$ to $\phi = +\infty$ (neglecting the delta function terms for the moment):

$$\frac{\partial}{\partial T}\int_{-\infty}^{\infty} d\phi P(\phi|T) = \frac{m_{\mathcal{P}}}{\sqrt{4\pi p}}\frac{1}{1-1/p}P(\phi|T) \qquad (3.20)$$
$$-\frac{d^2H^2(0)}{8\pi^2}\exp\Big[-\sqrt{\frac{16\pi}{p}}\frac{\phi}{m_{\mathcal{P}}}(1-\beta)\Big]\frac{\partial}{\partial\phi}\Big\{\exp\Big[-\sqrt{\frac{16\pi}{p}}\frac{\phi}{m_{\mathcal{P}}}\beta\Big]P(\phi|T)\Big\}.$$

If probability is conserved, the probability flux at $\phi = -\infty$ (the right hand side) must vanish. It does for $0 < \beta \leq 1$, but not for $\beta = 0$.

Although the $\beta = 0$ case is not of much physical interest since it corresponds to using the Hawking temperature at the end of the interval $(T, T+\Delta T)$ rather than at the beginning (Ito

formulation, $\beta = 1$) or in the middle (Stratonovich formulation, $\beta = 1/2$). For this case, the violation of probability conservation is given by,[35]

$$\int_{-\infty}^{\infty} d\phi\, P(\phi|T;\, T_0, \phi_0) = 1 - e^{-1/y}, \quad \text{for} \quad \beta = 0\ , \tag{3.21}$$

where y was given by (3.6c). The violation is extremely tiny, $\lesssim e^{-(10^{10})}$, for the $H(\phi_0)/m_{\mathcal{P}} \lesssim 10^{-5}$ allowed by microwave background constraints, but can be large for $H(\phi_0) \gtrsim m_{\mathcal{P}}$.

It is apparent from this argument that boundary effects require knowledge of the physics above an $m_{\mathcal{P}}^4$ energy density may play a role in determining the Fokker-Planck distribution. It was implicitly assumed in our derivation of (3.6) that (3.20) vanished. Langevin trajectories that diffuse to $\phi = -\infty$ should certainly be absorbed rather than be reflected. Although one can debate what the emission rate of trajectories from the quantum gravity era, the main possibilities are encompassed by the reflecting and absorbing conditions at $\phi = -\infty$. For absorbing boundary conditions, $P(\phi|T)$ should behave asymptotically as

$$P(\phi|T) \to \exp\Big[\sqrt{\frac{16\pi}{p}}\,\frac{\phi}{m_{\mathcal{P}}}\Big], \quad \text{as} \quad \phi \to -\infty. \tag{3.22}$$

The justification of this prescription is given in Appendix B, along with specific examples. Here we discuss the main results. The Green's function solution obeying (3.22) is similar to (3.6):

$$P^{abs}(\phi|T;\, T_0, \phi_0) \;=\; \sqrt{\frac{16\pi}{p m_{\mathcal{P}}^2}}\, y^{-1} e^{-(1+z^2)/y}\; z^{\beta+1}\, I_{1-\beta}(2z/y), \tag{3.23}$$

where y and z are defined by eqs.(3.6b,c). The interesting feature is that a Bessel function of order $1-\beta$ replaces the one of order $\beta - 1$ in (3.6a). Eq.(3.23) is valid for $0 < \beta < 1$, and the $\beta = 0, 1$ cases are found by taking appropriate limits. For $\beta \to 1$, the probability conserving solution (3.6) and the absorbing solution merge into the same distribution, indicating that boundary effects are unimportant for $\beta = 1$. This is another reason for favoring the $\beta = 1$ operator ordering choice. By contrast, as $\beta \to 0$, both solutions merge into an absorbing Green's function since $I_1(z) = I_{-1}(z)$, so in this case, it is not possible to conserve probability.

A nice choice for analytic simplicity is $\beta = 1/2$, since the modified Bassel functions which enter are $I_{-1/2}(x) = \sqrt{2/(\pi x)}\cosh(x)$ and $I_{1/2}(x) = \sqrt{2/(\pi x)}\sinh(x)$. The probability conserving solution (3.6),

$$P(\phi|T;\, T_0, \phi_0) = \sqrt{\frac{4}{y p m_{\mathcal{P}}^2}}\, z\Big[\exp - \Big[\frac{(z+1)^2}{y}\Big] + \exp\Big[-\frac{(z-1)^2}{y}\Big]\Big], \tag{3.24}$$

differs from the Green's function (3.23) for absorbing boundary conditions,

$$P^{abs}(\phi|T;\, T_0, \phi_0) \;=\; \sqrt{\frac{4}{y p m_{\mathcal{P}}^2}}\, z\Big[\exp\Big[-\frac{(z-1)^2}{y}\Big] - \exp\Big[-\frac{(z+1)^2}{y}\Big]\Big], \tag{3.25}$$

only by a appropriate minus sign. Eq.(3.24) is plotted for late times in Fig. 4. The tail is more pronounced than for the other cases shown. The absorbing boundary solution is plotted at several times for $H(\phi_0) = 3m_{\mathcal{P}}$ in Fig. 5. The final distribution has a total probability of 0.65:

about 1/3 of the paths have escaped from the system. It is still skew with a long tail extending to large energy densities.

Even for the case, $\beta = 1$, one should still be careful about boundary terms when $H(\phi_0) \approx m_P$. Although the total probability is indeed conserved, the mean and dispersion of ϕ pick up diffusion contributions from boundary terms. For example, multiplying the FP equation (3.4) for $\beta = 1$ by ϕ and integrating by parts twice yields an equation for the evolution of $\langle\phi\rangle$:

$$\frac{\partial\langle\phi\rangle}{\partial T} = \frac{m_P}{\sqrt{4\pi p}(1-1/p)} + \lim_{\phi\to-\infty}\frac{d^2H^2(0)}{8\pi^2}\exp\Big(-\sqrt{\frac{16\pi}{p}}\frac{\phi}{m_P}\Big)\,P(\phi|T_0,\phi_0)$$
$$= \frac{m_P}{\sqrt{4\pi p}(1-1/p)} + \frac{d^2H^2(\phi_0)}{8\pi^2}\sqrt{\frac{16\pi}{pm_P^2}}y^{-1}e^{-1/y}e^{-2(T-T_0)/(p-1)}.$$

The last term arises from the boundary term in the second integration by parts. It prevents the mean from evolving classically as a pure drift, and ensures that $\langle\phi\rangle > \phi_{cl}$ due to quantum diffusion.

In conclusion, we have found that different operator orderings give significantly different probability distributions if $H(\phi_0) \sim m_P$. In addition, the choice of boundary condition at $\phi = -\infty$ may have important effects for all cases except perhaps $\beta = 1$. For $0 < \beta < 1$, one can impose either a probability conserving boundary condition or a probability absorbing condition. If one chooses to disregard those stochastic paths that have reached arbitrarily large energy densities, then the latter is preferred. It does not appear that probability conserving solutions exist for $\beta = 0$. We favor $\beta = 1$ because the two different boundary conditions give the same answer.

IV. LATTICE SIMULATIONS OF THE LANGEVIN EQUATION

We saw in Sections II and III that when the initial conditions are considered as variables in the single point stochastic systems, some useful information about the power spectrum and other higher order correlations can be obtained. However, to solve the complete problem, full 3-dimensional realizations are required. In this section, we follow the classical drift and quantum diffusion of the scalar field on a comoving cubic lattice. Different points are correlated through the quantum noise terms given by the Fourier sum, eq.(2.10). Our numerical example is, once again, the system of a single scalar field with an exponential potential. This allows us to check our calculations with our exact solutions (3.6). In Sec. A, we reduce the equations of Sec. II to a form more convenient for numerical calculations and form the probability distribution for the field values at a single point through numerical integrations of the Langevin equation network for the lattice. In Sec. B, we display two 3-D simulations, the first a standard Gaussian run corresponding to our present horizon volume, and the second a non-Gaussian calculation of ultra-large scale structure.

A. Reduced Langevin Equation for Inflation with an Exponential Potential

For the case of inflation with an exponential potential, the Langevin equation (2.18) becomes

$$\Delta\phi(T,x^j) \equiv \phi(T+\Delta T,x^j) - \phi(T,x^j) = \frac{m_P}{\sqrt{4\pi p}}\frac{1}{1-1/p}\Delta T + \Delta S_\phi(T,x^j)\,. \qquad (4.1)$$

The noise in the momentum of the scalar field has been neglected and the attractor solution (3.2) of the separated Hamilton-Jacobi equation has been used. The variation $\Delta\alpha$ is related to

the variation $\Delta\phi$ and the time difference ΔT, so a separate stochastic equation for α does not have to be evolved.

The classical drift term is usually much larger than the quantum diffusion term, so it is useful numerically to subtract out as much of the drift as possible. In most cases, this involves a separate evolution of the stochastic equation for $\Delta\phi$ with drift forces only, and no diffusion, to define a smooth background level to subtract off. However, for the exponential case, we are in the fortunate position of having a drift velocity which is independent of ϕ so there is a universal drift which is linear in T that can be immediately subtracted. In terms of the dimensionless variable

$$\chi = (\phi - \phi_{cl})/H(\phi(0)) \tag{4.2}$$

describing the deviation from the classical trajectory, (3.3), the Langevin equation has only a time-dependent diffusion term:

$$\Delta\chi = \Delta\mathcal{S}_\phi = d(\phi)e^{-T/(p-1)}\exp\Big(-\sqrt{\frac{4\pi}{p}}\frac{H(\phi_0)}{m_{\mathcal{P}}}\chi\Big)\sum_{e^T\le|\mathbf{k}|<e^{T+\Delta T}}\Big[\frac{a(\mathbf{k})}{\sqrt{2k^3}}e^{i\mathbf{k}\cdot\mathbf{x}}\Big]. \tag{4.3}$$

In the following, we take the correction factor $d(\phi)$ to be unity. Since there is no drift term to integrate numerically between stochastic impulses, this system is one of the easiest to compute. However, one of the possible origins for non-Gaussian fluctuations, nonlinear drift evolution, is therefore absent. Thus, for this system, we can get non-Gaussian statistics only through the nonlinear mode-mode coupling in the noise term associated with the exponential.

If one is interested in the distribution of fluctuations at a single point, say $x = 0$, then the Langevin equation involves only a single Gaussian random variable, $A(T)$, for each value of T:

$$\Delta\chi = \frac{(\Delta T)^{1/2}}{2\pi}e^{-T/(p-1)}\exp\Big(-\sqrt{\frac{4\pi}{p}}\frac{H(\phi_0)}{m_{\mathcal{P}}}\chi\Big)A(T)\,. \tag{4.4}$$

$A(T)$ has been defined to have unit dispersion (noting that $\Delta T/(2\pi)^2$ is the variance of $\sum_{e^T\le|k|<e^{T+\Delta T}} a(k)/\sqrt{2k}$ Also, $A(T)$ and $A(T')$ are statistically independent for $T \neq T'$.

The comoving coordinates, x^i, of each spatial point are labelled by three integers, n^1, n^2, n^3 with $x^i = L_c n^i/N_L^{1/3}$, where L_c is the comoving box size. The comoving vectors $\vec{k}$ that appear in the Fourier sum, eq.(4.2), are also labelled by 3 integers, m_1, m_2, m_3, with $k_i = k_{min}(m_i - N_L^{1/3}/2)$, where the minimum length of the wavevector is $k_{min} = 2\pi/L_c$. When the calculation begins, one does not know the size of the lattice as measured today, because it depends upon when the scalar field reheats and how much entropy is generated. The actual length scale today will be discussed later. For the purposes of the calculation we set $k_{min} = 1$.

As explained in Sec. II.D, we assume that the entire lattice system is homogeneous at T_0, which we take to be zero since $k_{min} = 1$. Thus $\chi(n^1, n^2, n^3, 0)$ starts at 0. Therefore the uniform initial Hubble parameter, $H(\phi_0)$, is all that is required to set the initial conditions for the simulation. Thus all inhomogeneities in the system are the direct result of quantum noise terms that leave the horizon after T_0. In the j^{th} time step, T_j to T_{j+1}, where $T_j \equiv (j-1)\Delta T$, if the comoving wavenumber has a magnitude $|\mathbf{k}|$ that falls within the range e^T to $e^{T+\Delta T}$, then the scalar field again obtains a kick given by (4.3):

$$\chi(n^1, n^2, n^3, T_{j+1}) = \chi(n^1, n^2, n^3, T_j) + \Delta\mathcal{S}_\phi(\chi(n^1, n^2, n^3, T_j), T_j).$$

Notice that the amplitude of the stochastic kick is evaluated at T_j rather than in between T_j and T_{j+1}. This corresponds to our choice of Ito ordering[36] for the stochastic noise evaluation

(see Appendix A). One could instead evaluate the stochastic noise term at intermediate steps during the time interval, which leads to different Fokker-Planck equations (Sec. III.B.4) as well as different lattice simulation results than those shown here, but we exclusively adopt Ito ordering here. If the drift must be explicitly calculated as well, which is not required for this exponential potential model, the classical propagation of the field from $\chi(n^1, n^2, n^3, T_j)$ to $\chi(n^1, n^2, n^3, T_{j+1})$ occurs first, then the stochastic impulse is added.

The stochastic noise term modulates the Gaussian-distributed Fourier sum by the spatial and temporal dependence encoded in the local value of the Hubble parameter. The complex random fields $a(\mathbf{k})$ must be properly normalized and symmetrized. We use

$$a(\mathbf{k}) = a_R(\mathbf{k})/\sqrt{2} + ia_I(\mathbf{k})/\sqrt{2}$$

where a_R and a_I are random numbers calculated from a Gaussian random number generator with unit dispersion, $< a_R^2 >=< a_I^2 >= 1$. We also require that the Fourier sum be real, hence $a(m_1, m_2, m_3) = a(N - m_1, N - m_2, N - m_3)$, unless one or more of the m_i equals N, in which case $a(m_1, m_2, m_3)$ is real, with unit dispersion.

The time step ΔT is chosen by requiring that the increment of χ in going from T to $T + \Delta T$ be less than some ϵ:

$$\Delta T < 4\pi^2\epsilon^2 e^{2T/(p-1)} \exp(\sqrt{16\pi/p} H(\phi_0)\chi). \tag{4.5}$$

If $\epsilon = 0.2$ and if the argument in the second exponential is always small compared to one, then $\Delta T \leq 0.2$ is usually more than sufficient for the entire calculation. However, in Sec.B.2, we also consider the situation when $H(\phi_0) \approx m_{\mathcal{P}}$. In this case, some points receive several negative kicks in rapid succession so the value of the Hubble parameter may become enormous. The time step given by eq.(4.5) depends exponentially on the value of the scalar field, which makes the system numerically unstable. It is computationally impractical to continually diminish the time step. We therefore choose to monitor only those points with χ larger than a threshold value χ_{cut}:

$$\chi > \chi_{cut} \equiv -5\sqrt{\frac{p-1}{8\pi^2}}. \tag{4.6}$$

χ_{cut} is five times the initial dispersion that one would calculate if the fluctuations were linear, eq.(3.14). Thus, at those points for which χ decreases below χ_{cut}, we artificially set it equal to χ_{cut} and we do not evolve it further. This is therefore an absorbing barrier boundary condition at χ_{cut}. For $H(\phi_0) = 1.0 m_{\mathcal{P}}$ with $\epsilon = 0.2$, the time step is chosen to be the same at all points in the lattice, $\Delta T = 0.01$.

As a check of the code, we numerically integrated the Langevin equation governing fluctuations without spatial correlations, eq.(4.4). Sample trajectories are shown in Fig. 6a for the $H(\phi_0)/m_{\mathcal{P}} = 10^{-5}$, $p = 5$ case. The fluctuations grow rapidly, reach their maximum amplitude at about $T = 5$, then essentially stop growing because the stochastic force decreases linearly with the Hubble parameter. Fig.6b depicts the final histogram for 50,000 paths and compares with the exact solution, demonstrating excellent agreement.

B. 3-D Lattice Simulations

1. Gaussian Simulation

A two dimensional slice of a 64^3 lattice simulation is shown in Fig. 7a for the single scalar field model with an exponential potential and initial Hubble parameter $H(\phi_0)/m_{\mathcal{P}} = 10^{-5}$. Because the contours shown, $\Delta\phi/\sigma \equiv (\phi - \langle\phi\rangle)/\sigma = -2, -1, 0, 1, 2$, where σ is the dispersion

in the scalar field, are so densely packed we also show just the -2σ contours in Fig. 8a; there are 91 points with ϕ below this, compared with the prediction of 94 for an average Gaussian map of this size. Fig. 7 gives a rough indication of what a large angle microwave background map would look like for this model, with an *rms* amplitude of $\Delta T_{cmb}/T_{cmb}$ being $\sim 10^{-5}$, since $\Delta T_{cmb}/T_{cmb}$ is basically proportional proportional to $\Delta\phi$ through eq.(3.12b), apart from the caveats of Sec. II.G. Since the field is very well approximated by a Gaussian-distribution, a fast Fourier transform on the fluctuation spectrum ($\mathcal{F}^{1/2} \propto k^{-1/(p-1)}$, given by eq.(3.18)) is a much simpler way to simulate the field than this Langevin network integration approach. However our method can be applied to the generation of non-Gaussian patterns that arise in stochastic inflation models.

2. Non-Gaussian Simulation

A two-dimensional slice of a 64^3 non-Gaussian lattice calculation is shown in Fig. 7b. Since significant non-Gaussian statistics only arise when the initial value of the Hubble parameter is comparable to the Planck scale, we have taken $H(\phi_0) = m_{\mathcal{P}}$. The map of scalar field fluctuations for -2,-1σ contours (solid) and 0,1,2σ contours (dashed) is shown in Fig. 7b, and for -2σ fluctuations only in Fig. 8b. A histogram of the scalar field deviations from the mean is depicted in Fig. 9b. As discussed in Sec. III.B.3, the distribution of scalar field values in Fig. 9b is skewed. The distinctive tail to negative $\Delta\phi$ dominates the appearance of the contour map. Since only stochastic noise over a 64^3 reciprocal lattice in k-space was used with our algorithm, the lattice simulation, which began at $T = 0$, is depicted at a time $T_f \approx 4$, when all the waves are used up. (For a more efficient algorithm see ref.24.) The ϕ–map is in initial comoving coordinates $\vec{r}$, not final physical coordinates $\vec{x}$, where the relation is $\vec{x} = \exp[\alpha(\vec{r}, T_f) - \alpha_0]\,\vec{r}$. Since the fluctuations in α are nonlinear, this distortion of the lattice is essential in describing the metric (*i.e.*, α) fluctuations at the observable final points: $\alpha(\vec{x}, T_f)$ in the distorted lattice obeys a very complex relation to $\alpha(\vec{r}, T_f)$.

Low energy density regions are scarcer than in the Gaussian case and steep high peaks are much more common, with 192 points below -2σ in the map compared with 91 Fig.7a. The gross features of the map are already evident from the Green's function, which is a useful first quantity to evaluate for more realistic non-Gaussian fluctuation models.

Contour plots for a simulation with $H(\phi_0) = 3m_{\mathcal{P}}$ are similar to those of Fig. 7b,8b except that the high energy density regions are more numerous with steeper $-\phi$ peaks.

The $H(\phi_0) = m_{\mathcal{P}}$ example is marginally unstable numerically: $\frac{1}{2}\%$ of the initial points were discarded in the leftmost bin of Fig. 9b, since they were absorbed according to our criterion (4.6). Even so, the numerical calculation agrees well with the exact solution. The Langevin system becomes very unstable for much higher initial values of the initial Hubble parameter. Even for $H(\phi_0) = 3m_{\mathcal{P}}$, about 10% of the paths have to be discarded. The problem is the exponential dependence of the stochastic force on $-\phi$, so one would require an exponentially small time step according to (4.5) to monitor the evolution accurately. The exact Fokker-Planck solutions of Sec. III.B.4, which show the importance of diffusion to large $-\phi$ for $H(\phi_0) \gtrsim m_{\mathcal{P}}$, illustrate why we should expect difficulties following the Langevin system in this large $H(\phi_0)/m_{\mathcal{P}}$ regime.

The non-Gaussian statistics of the map 7b are not of relevance for observed cosmic structures. We estimate the present size of the lattice which crossed the horizon during inflation when $H \approx m_{\mathcal{P}}$ assuming that the size of the lattice for the current comoving Hubble volume must have had $H(\phi_0)/m_{\mathcal{P}} \approx 10^{-5}$ to satisfy $\Delta T_{cmb}/T_{cmb} \approx 10^{-5}$. Our time choice T is $\ln k_H$,

where k_H was the comoving wavenumber at horizon crossing, $k_H/(He^{\alpha}) = 1$. Along a classical trajectory, the Hubble parameter varies in time as

$$H/H' = \exp\left[-\sqrt{\frac{4\pi}{p}}(\phi - \phi')/m_{\mathcal{P}}\right] = \exp\left[-(T - T')/(p-1)\right] .$$

The ratio in size between a Universe which left the horizon during inflation with $H' = m_{\mathcal{P}}$ and one which left with $H = 10^{-5} m_{\mathcal{P}}$ is

$$\frac{k_H}{k'_H} = e^{T-T'} = \left(\frac{H'}{H}\right)^{p-1}, \quad \approx 10^{22} \quad \text{for} \quad p \approx 5 .$$

Although this estimate is quite p sensitive, it is clear that $H' = m_{\mathcal{P}}$ corresponds to a length scale very much larger than our current observable patch of the Universe. Larger p makes matters worse, and much smaller p violate microwave background limits. Hence, at least for this single scalar field model, the effects of nonlinear evolution at large wavelengths has no observable consequences. We emphasized these models in this paper because they were the simplest for which nonlinear mode-mode coupling could be computed.

The free parameter p that controls the steepness of the exponential potential is strongly constrained by large angle microwave background constraints. At the moment, the best large angle limits come from the Soviet RELICT experiment, but the COBE satellite should soon surpass its sensitivity. The scale-invariant Cold Dark Matter (CDM) model ($p \to \infty$) is a factor of $2.4 b_\rho$ below the RELICT constraint, where the biasing factor b_ρ is between about 1 and 2.5 to generate the observed galaxy clustering. According to eq.(3.18), inflation with an exponential potential produces a fluctuation spectrum $\mathcal{F}^{1/2} \propto k^{-1/(p-1)}$. A reasonable estimate of the properly normalized fluctuation spectrum for smaller p is to multiply the scale invariant CDM model by $(k/k_G)^{1/(1-p)}$, where the normalization scale $k_G^{-1} = 10$ Mpc is chosen to fix the density perturbations to the observed galaxy clustering level. To avoid too much power at large scales, p cannot be too small. The rough estimate

$$\left(\frac{k^{-1}}{k_G^{-1}}\right)^{1/(p-1)} \lesssim 2.4 b_\rho$$

for $k^{-1} \approx 10^4$ Mpc, the current horizon scale, gives $p \gtrsim 5$ for $b_\rho \lesssim 2$. More sophisticated calculations give approximately the same constraint on p.[37]

V. DISCUSSION AND SUMMARY

The main objectives of this paper were to develop a formalism for efficiently calculating the fluctuations that develop in stochastic inflation, and to illustrate how it works for a single scalar field in an exponential potential, which is perhaps the simplest (often analytically tractable) inflation model. In SB1,[12] we showed that a diagonal metric of the form $ds^2 = -N^2(T, x^i)dT^2 + e^{2\alpha(T,x^i)}(dx^2 + dy^2 + dz^2)$ adequately describes the evolution of inhomogeneous background fluctuations that have been smoothed on scales smaller than the Hubble radius, up to second order in the spatial gradients. The ADM (3+1 split) equations for the inhomogeneous background fields reduce to energy and momentum constraint equations, and evolution equations first order in time for the physical variables, $\bar{\phi}_j$, $\bar{\alpha}$ and their corresponding momenta, $\bar{\Pi}^{\phi_j} = \dot{\bar{\phi}}_j/\bar{N}$, $\bar{H} = \dot{\bar{\alpha}}/\bar{N}$. To the evolution equations we add classical stochastic noise terms which model quantum fluctuations which have crossed the horizon. The constraint equations do not contain noise terms because they do not explicitly contain time

derivatives. The solution of the ADM momentum constraint equation gives the Hubble parameter $\bar{H} \equiv \bar{H}(\bar{\phi}_j(T, x^i), T)$ as a function of the local value of the scalar fields as well as the time parameter. Substitution into the energy constraint leads to a partial differential equation for H, the separated Hamilton-Jacobi equation. Although the solutions generally depend upon arbitrary parameters, all solutions rapidly approach one another during inflation, resulting in a memory loss so that H is a function only of the local field strengths ϕ_j. Such solutions would be attractors.

The dominant behavior after a stochastic impulse is for the disturbed system to rapidly decay to the attractor, and the subdominant behavior is for the field to drift down the potential along the attractor solution. It is therefore highly advantageous to adopt an approximation that removes the unwanted decaying mode at the outset, for both numerical and analytic reasons. By requiring $\bar{H}$ to be a function of ϕ_j only, we have done this. This key approximation avoids the unpleasantness of trying to construct a numerical algorithm to do it in the full Langevin network. As well, the scalar field momenta $\bar{\Pi}^{\phi_j} = -(m_p^2/(4\pi))\,\partial\bar{H}(\phi_j)/\partial\phi_j$ are also just functions of the local field strengths ϕ_j. Although much more general than the usual slow roll-over relation for $\bar{\Pi}^{\phi_j}$, it has some of the same effects: the evolution equations for the momenta $\bar{\Pi}^{\phi_j}$ and $\bar{H}$ are dropped from the network, leaving only (first order) stochastic evolution equations for ϕ_j and α at each spatial point. With a choice of time variable T which is a function of ϕ_j and α, one of these becomes redundant. However, for this approximation to be really useful, we would ideally like to have an analytic attractor, such as we get for slow rolldown or in the exponential potential case. For more general situations, one could in principle still use the Hamilton-Jacobi method; in practice, it is better to just integrate the equations, including the momentum evolution equation.[24] As well, although our approximation is excellent for the single scalar field model, it can sometimes fail with many scalar field degrees of freedom.

The time surface across which the communication between short wavelength and long wavelength fields occurs is obviously a difficult issue. We showed that the high spatial frequency WKB solution on an inhomogeneous long wavelength background has the same form as the WKB solution on a homogeneous background if the local background conformal time $\int d\alpha (He^{\alpha})^{-1}$ is used. Although this suggests conformal time is a preferred time variable, we found it more convenient to use the related variable $T = \ln(H(\phi_j)e^{\alpha})$ instead. The obvious interpretation is that $T = \ln k_H$, where k_H is the comoving wavenumber of the short wavelength fluctuations that are crossing the horizon. This time coordinate actually breaks down at the acceleration/deceleration boundary marking the end of inflation, so to follow the oscillating and 'reheating' phase, it is necessary to change hypersurfaces, *e.g.*, to uniform Hubble surfaces — with the time H — upon which the evolution of the long wavelength metric perturbations is simple.[28,8]

The high spatial frequency WKB solution for wavenumber k has an *rms* amplitude for the scalar field perturbations given by the local Hawking temperature when evaluated at $k = k_H$, giving the amplitude of the waves. The linearization approximation at subhorizon scales ensures that each new wave coming across the horizon is uncorrelated with the last, making the stochastic noise term a Markov process. Choosing the time as k_H implies, within the high frequency linearization approximation, that the stochastic noise is Gaussian-distributed. This would not be true on other hypersurfaces.[24] The noise term really requires full integration of the linear fluctuations on an inhomogeneous background until transients have died away, so the matching is really best done when $k = \epsilon k_H$, where $\epsilon < 1$, as Starobinski[10] emphasized. We only approximately included this effect here (the parameter d of §III), but address it more fully in ref.24.

The coupling of the points that leads to spatial correlations occurs only through the stochastic impulses since background field gradients are of second order in the evolution equations and have therefore been dropped. Although these impulses are Gaussian-distributed at each point, the nonuniformity of their Hawking temperature amplitude on the T hypersurfaces implies that

each stochastic kick that the lattice receives is a non-Gaussian field, and the sum of these kicks will be even more so. Another mechanism by which non-Gaussian perturbations can arise is through nonlinearities associated with the drift force, even if the stochastic kicks are Gaussian fields. For the exponential potential model, the latter is not relevant, but for general potentials both effects would be inextricably coupled.

What we wish to compute is what we can observe, the structure within our local observable patch of the Universe, encompassing the current Hubble volume. We can split the calculation of the fluctuations within this region into two steps. In the first step the ultra-large scale structure (ULSS) of the Universe is computed to obtain the starting conditions for our patch. Although there is ULSS, which is non-Gaussian, exhibiting all of the remarkable features predicted of eternal inflation, we expect that this will lead to relatively uniform starting conditions for the field and metric structure over our patch. There may be pathologies with a nonlinear coupling leading to some shorter distance structure from a steepening of the ULSS, but it is certainly not expected in the generic case, *e.g.*, for the exponential potential model. Thus, from the point of view of our own observable large scale structure, the ULSS enters only as a set of N background field strengths, ϕ_{j0}, and one only needs the one-point probability distribution, say $P(\phi_{j0}|T_0)$. One may debate what the best time hypersurface is to specify the initial conditions for our local patch. The difficulty here is that we do not really know that a patch is viable until after it has been evolved. (In practice, the fluctuations are so small within our patch that we do in fact have a very good idea of how to proceed, guided by linear perturbation theory.)

With the homogeneity assumption, the probability of the field at a given point of our patch begins as a delta function, $\lim_{T\to T_0} P(\phi_j|T;T_0,\phi_{j0}) = \delta^n(\phi_j - \phi_{j0})$, so the Fokker-Planck solution is the Green's function. Thus the field value at a point has a distribution which is

$$P(\phi_j|T) = \int d^n\phi_{j0}\, P(\phi_j|T;T_0,\phi_{j0})\, P(\phi_{j0}|T_0),$$

and this is non-Gaussian, but that is only because the homogeneous initial conditions are. If the *observable* constraint is imposed to select only those initial parameters, $\phi_{j0}, j = 1,..,n$, which lead to microwave background anisotropies consistent with the observational bounds, a severe further selection is imposed on ϕ_{j0}. That data enters in the conditioning is fundamental to understanding stochastic inflation, since, unlike in linear perturbation theory, there is no unique global homogeneous background value unresponsive to backreaction as quantum modes are added. To see that some conditioning is essential, we note that we must, at the very least, select only those patches of the Universe that reheat, and reject those regions that eternally inflate. For a single scalar field, we used $H(\phi_0)$ to characterize of the initial amplitude and saw that to explain the level of large scale structure we observe in the galaxy distribution and the lack of structure in the microwave background,we must have $H(\phi_0) \sim 10^{-5} m_P$. To pin it down precisely would require detailed simulation and confrontation with the cosmic structure data.

We have also seen the central role that the one-point probability distribution plays as a function of initial constraint conditions. This conditioning is an essential requirement to relate stochastic inflation calculations with observations. We showed that, by considering the probability and the *rms* fluctuations in α as a function of the average physical volume of a patch, we can find a quantity analogous to the power spectrum that describes how the fluctuation amplitude changes with scale.

The exponential potential model has the essence of the standard inflation picture for one scalar field in it, and the analytic results provide considerable insight to what will occur with other potentials. For example, the analytic one-point distributions give a clear indication of the generic nature of eternal inflation.[17] They also serve as a very useful guide for deciding how to

contend numerically with the problem in the simulations of stochastic inflation maps when the starting conditions have $H(\phi_0) \sim m_{\mathcal{P}}$.

Although the exponential potential model has been very instructive, we emphasize that the reheating issue cannot really be ignored in stochastic inflation, since it defines the hypersurface that all the stochastic trajectories must reach for the patch to be a contender for our local region of the Universe. (A simple reheating criterion might be that the hypersurface is one with a critical Hubble parameter H_{reh}, when $H = (3/2)^{1/2} H_{SR}$, where H_{SR} is the slow roll Hubble parameter.) To determine the mapping of our observed scales to the initial comoving lattice positions, we need reheating, so that we can work backwards using the ~ 60 e-foldings after the acceleration/deceleration boundary has been reached in conjunction with the inflation e-foldings to get our current horizon scale.

The key simple image to draw from this paper is of the ULSS distribution of Fig.7b on unobservably large scales, with its high energy density non-Gaussian mountain peaks, and the zoomed-in structure of Fig.7a for our observable patch corresponding to an infinitessimal subscale of Fig.7b. Fig.7a is Gaussian, and, to satisfy microwave constraints, only a small subset of regions of the ULSS will do. Note that even with a hypersurface change, Fig.7a will remain Gaussian. However, hypersurface changes for the ULSS would give vastly different images. Indeed, if Figure 7b were viewed in physical space rather than initial comoving space, we would see a large distortion of the patch from a square lattice. On T surfaces, the peaks would become narrower. However, on another hypersurface, we would see huge regions of high α because those comoving regions with very high α have the local space stretched out. All these problems are of second order, so were never encountered in linear perturbation theory treatments.

Nonlinear interaction is required to get non-Gaussian primordial fluctuations from inflation. However, the specific method for generating non-Gaussian fluctuations used in this paper will not be able to produce *observable* non-Gaussian fluctuations. This result seems to be generic for single field inflation models that satisfy the microwave background constraints. However, there are a number of possibilities that could give rise to nonlinear interactions that have not been well studied and are not, as yet, included in our stochastic framework. For example, the linear WKB treatment of quantum fluctuations at short distances may be too naive and they really are non-Gaussian. There are various fundamental physical scales that could be responsible for leaving nonlinear imprints within the final fluctuations. Three scales are of relevance for chaotic inflation: (1) the Hubble scale, $H \approx 10^{-5} m_{\mathcal{P}}$, set by the level of fluctuations to form galaxies, and already discussed here; (2) the grand unified scale $\sigma \approx 10^{-4} m_{\mathcal{P}}$, set by particle physics; and (3) the Planck scale $m_{\mathcal{P}} = G^{-1/2}$. Although GUT scale physics led to the development of the inflation paradigm, it is quite possible that it plays no role at all. We know, however, that the Planck scale must be important since gravity is fundamental to inflation. For a $\lambda\phi^4/4$ potential, the scalar field must start at approximately $5 m_{\mathcal{P}}$ for our patch of the Universe in order that it inflates sufficiently, a result independent of the self-coupling λ; and much higher scalar field values are contemplated in chaotic inflation, possibly with energy densities up to $m_{\mathcal{P}}^4$. We believe that the stochastic inflation formalism provides an excellent framework within which to explore the different sources of nonlinearity, with the Langevin network acting like transport equations carrying short distance physics across the Hubble radius to eventual confrontation with observables.

So far, the non-Gaussian fluctuations from inflation that have been discussed in the literature are like the ones here, of ultra-large scale, or are a result of large fluctuations in a subdominant scalar field, as in the axion models,[18,19] or as a result of building in judiciously arranged structure on the potential surface for models with more than one scalar field.[39,8,40] Although the nonlinear scales for the latter are so far put in by hand, the form that the fluctuations take is quite instructive,[39] and it is to the simulation of such models, using an extension of the methods in this paper, that we turn in Bond and Salopek.[24]

We thank Jim Bardeen and Alexei Starobinski for useful discussions. D.S.S. was funded by NSERC of Canada, the U.S. Department of Energy, and NASA at Fermilab (Grant No. NAGW-1340). J.R.B. was supported by NSERC and the Canadian Institute for Advanced Research.

APPENDIX A: THE FOKKER-PLANCK EQUATION DERIVED FROM THE LANGEVIN EQUATION

In this Appendix, we review how one derives the Fokker-Planck equation from the Langevin equation (see *e.g.*, Chandrasekhar[38] and van Kampen[36]) and discuss how it depends upon the treatment of the time integral of the stochastic force. Consider the Langevin equation for a single variable x,

$$\dot{x} = f(x) + Q(x,t), \tag{A1}$$

where the stochastic noise term is uncorrelated at different times:

$$< Q(x,t)Q(x,t') >= \sigma^2(x)\delta(t-t'). \tag{A2}$$

Thus for very short time intervals Δt, the distance traversed is a random walk plus a drift, $< (\Delta x - f(x)\Delta t)^2 >= \sigma^2(x)\Delta t$. To construct the associated Fokker-Planck equation, one needs the short time Green's function. One possible form would be

$$G(x, t+\Delta t|x', t) = [\sigma^2(x')\Delta t]^{-1/2}\, g\Big[\frac{x - x' - f(x')\Delta t}{\sigma(x')\Delta t^{1/2}}\Big], \tag{A3}$$

where the functional form of g depends upon the statistics of Q. G approaches an initial delta function distribution as $\Delta t \to 0$, and it preserves probability, $\int G(x, t+\Delta t|x', t)dx = 1$. The function $g(s)$ peaks about $s = 0$ and has its first few moments given by

$$\int g(s)ds = 1, \quad \int sg(s)ds = 0, \quad \text{and} \int s^2 g(s)ds = 1. \tag{A4}$$

If Q is Gaussian-distributed, as for our case, then G is Gaussian. However, even if it is not, the results are independent of the higher moments of g. With the form (A3), the discrete version of the Langevin equation (A1) over a time interval Δt is (with $x = x(t+\Delta t)$, $x' = x(t)$)

$$x(t+\Delta t) = x(t) + f(x(t))\Delta t + \sigma(x(t))[(\Delta t)^{1/2}\, s]\ .$$

$f(x(t))\Delta t$ describes the classical drift in time Δt and $\sigma(x(t))(\Delta t)^{1/2}\, s$ is the diffusion contribution, where s is Gaussian deviate (with unit dispersion). This form of the discrete Langevin equation with the diffusion term evaluated at the beginning of the interval is called the Ito form. We can consider a more general form:

$$\begin{aligned} x(t+\Delta t) = x(t) &+ \sum_b w_b f[\beta_b x(t) + (1-\beta_b)x(t+\Delta t)]\Delta t \\ &+ \sum_b w_b \sigma[\beta_b x(t) + (1-\beta_b)x(t+\Delta t)]\ [(\Delta t)^{1/2}\, s]\ , \end{aligned} \tag{A5a}$$

where the weights w_b and β_b describe how the time integrals in (A1) are to be approximated over the interval Δt. They lie in the interval 0 to 1 and satisfy the identity $\sum_b w_b = 1$. We let $\bar{\beta} \equiv \sum_b w_b\beta_b$. We can expand the functions f and σ and keep terms of at most first order in Δt. The drift term is already of that order. Only the noise part must be treated carefully:

the expansion of σ contains a term linear in Δx, which has a stochastic contribution of order $(\Delta t)^{1/2}$, which multiplies the order $[(\Delta t)^{1/2}\, s]$ term already there to yield a term of order Δt. Thus,

$$x(t+\Delta t) = x(t) + f(x(t))\Delta t + \sigma(x(t))(\Delta t)^{1/2}\, s + (1-\bar{\beta})\frac{\partial \sigma}{\partial x}(x(t))\,\Delta x\,[(\Delta t)^{1/2}\, s]\ .$$

A shortcut to the correct form of the stochastic equation uses the Ito calculus,[36] in which the square of the 'Weiner increment' $[(\Delta t)^{1/2}\, s]$ is taken to be Δt, so (A5a) becomes

$$x(t+\Delta t) = x(t) + \Big[f(x(t)) + \frac{1}{2}(1-\bar{\beta})\frac{\partial \sigma^2}{\partial x}(x(t))\Big]\,(\Delta t) + \sigma(x(t))\,[(\Delta t)^{1/2}\, s]\ . \qquad (A5b)$$

The different approximations to the time integral of (A1) over Δt correspond to slight modifications of the drift force, $f \rightarrow f_\beta = f + (1/2)(1-\bar{\beta})(\partial\sigma^2/\partial x)$. The Ito version of the stochastic equation has $\bar{\beta} = 1$. The Stratanovich version evaluates σ at the intermediate point $(x(t) + x(t+\Delta t))/2$, hence $\bar{\beta} = 1/2$.

Given an initial probability distribution, $P(x,t)$, one may determine the distribution at a little later time $t+\Delta t$ by integration over the Green's function,

$$P(x, t+\Delta t) = \int G(x, t+\Delta t | x', t) P(x', t) dx'\ . \qquad (A6)$$

The integral may be evaluated by making a change of variables from x' to

$$s = \frac{x' + f_\beta(x')\Delta t - x}{\sigma(x')\Delta t^{1/2}}. \qquad (A7)$$

We wish to calculate the probability function to second order in $(\Delta t)^{1/2}$. We invert (A7) to this order, by consider iterative approximations of

$$x' = x + \sigma(x')\Delta t^{1/2} s - f_\beta(x')\Delta t,$$

which gives $x' = x + \sigma(x)\Delta t^{1/2} s$ to first order in $(\Delta t)^{1/2}$, and

$$x' = x + \sigma(x) s \Delta t^{1/2} + \Big[\frac{s^2}{2}\frac{\partial(\sigma^2)}{\partial x} - f_\beta(x)\Big]\Delta t \qquad (A8)$$

to second order. Similarly, to second order the volume element is

$$\frac{dx'}{\sigma(x')\Delta t^{1/2}} = ds\Big[1 + \frac{s}{2}\Delta t^{1/2}\frac{\partial \sigma}{\partial x} + \Delta t\Big(-\frac{\partial f_\beta}{\partial x} + \frac{s^2}{2}\frac{\partial^2(\sigma^2)}{\partial x^2}\Big)\Big]. \qquad (A9)$$

All the functions on the right are evaluated at x. With these results, (A6) can be integrated to second order in $(\Delta t)^{1/2}$, yielding the Fokker-Planck equation:

$$\frac{\partial P}{\partial t} = -\frac{\partial}{\partial x}\Big[f_\beta(x)P\Big] + \frac{1}{2}\frac{\partial^2}{\partial x^2}\Big[\sigma^2(x)P\Big]. \qquad (A10)$$

Note that we could have derived the f_β term by expanding σ that entered the Green's function (A3) to linear order. This is the 'operator ordering' ambiguity. Note that when the form of f_β is substituted in (A10), we get

$$\frac{\partial P}{\partial t} = -\frac{\partial}{\partial x}\Big[f(x)P\Big] + \frac{1}{2}\frac{\partial}{\partial x}\sigma^{2(1-\beta)}\frac{\partial}{\partial x}\Big[\sigma^{2\beta}(x)P\Big]. \qquad (A11)$$

The same derivational approach applies to a system of Langevin equations

$$\dot{x}_j = f_j(x_k) + Q_j(x_k,t), \quad \text{with} \quad < Q_i(x_k,t)Q_j(x_k,t') >= (\sigma^2)_{ij}(x_k)\delta(t-t').$$

For $\beta = 1$, we have a Fokker-Planck equation which can be applied to many scalar fields and even for many spatial points:

$$\frac{\partial P}{\partial t} = -\sum_j \frac{\partial}{\partial x_j}[f_j(x_k)P] + \frac{1}{2}\sum_{i,j}\frac{\partial}{\partial x_i}\frac{\partial}{\partial x_j}[(\sigma^2)_{ij}(x_k)P]. \qquad (A12)$$

In the body of the paper we denote $\bar{\beta}$ by β.

APPENDIX B: BOUNDARY CONDITIONS FOR THE FOKKER-PLANCK EQUATION

We expand on the assertion made in Sec. III.B.4 that some solutions of the Fokker-Planck equation depend on the choice of boundary conditions at $\phi = -\infty$. There are two types of boundary conditions that are of interest: (1) probability preserving and (2) probability absorbing. To discuss these conditions, it is useful to make several changes of variables of the Fokker-Planck equation (3.4) for an exponential potential. In this Appendix, we use P_T to denote $P(\phi|T)$.

The drift term can be removed from (3.4) by using the z of eq.(3.6b) in place of ϕ. The derivatives transform according to

$$\Big(\frac{\partial}{\partial T}\Big)_\phi = \Big(\frac{\partial}{\partial T}\Big)_z - \frac{z}{p-1}\Big(\frac{\partial}{\partial z}\Big)_T, \quad \Big(\frac{\partial}{\partial \phi}\Big)_T = \sqrt{\frac{4\pi}{pm_p^2}}z\Big(\frac{\partial}{\partial z}\Big)_T,$$

so the Fokker-Planck equation becomes

$$\frac{\partial P_T}{\partial T} = \frac{d^2}{2p\pi}\frac{H^2(\phi_0)}{m_p^2}e^{-2(T-T_0)/(p-1)}\,z\frac{\partial}{\partial z}\Big[z^{2\beta-1}\frac{\partial}{\partial z}\Big(z^{-2\beta}P_T\Big)\Big].$$

In terms of the time parameter y introduced in (3.6c) as well as a new function

$$R(y,z) = \sqrt{\frac{pm_p^2}{4\pi}}z^{-1}P_T, \qquad (B1)$$

we can rewrite this as

$$\frac{\partial R}{\partial y} = \frac{1}{4}\frac{\partial}{\partial z}\Big[\frac{(1-2\beta)}{z}R + \frac{\partial R}{\partial z}\Big], \qquad (B2)$$

which is symmetric under the parity transformation, $z \to -z$,

To obtain the probability conserving boundary condition, we integrate (B2) over z from 0 to ∞:

$$\frac{\partial}{\partial y}\int_0^\infty R dz = -\frac{1}{4}\Big[\frac{(1-2\beta)}{z}R + \frac{\partial R}{\partial z}\Big]_{z=0}. \qquad (B3)$$

The right hand side is the probability flux at $z = 0$. If the total probability is preserved, it must vanish. This condition is met if the probability function is asymptotically a power-law, $R \to z^{2\beta-1}$ for $0 < \beta < 1$. For example, the solution (3.6) meets this condition.

The condition corresponding to the boundary absorbing any stochastic paths incident upon it is more complex. We first consider a simple example, with $\beta = 1/2$ so that eq.(B2) reduces to a simple diffusion equation. The fundamental Green's function, with no boundary constraints, is the usual well known Gaussian

$$R^{fund}(y, z; y_0, z_0) = \frac{1}{\sqrt{\pi y}} \exp\Big[-\frac{(z-z_0)^2}{y}\Big]. \qquad (B4)$$

From now on, we shall let $z_0 = 1$. If the boundary at $z = 0$ reflects all paths that reach it, then the resulting Green's function may be found by adding an image source at $z = -z_0 = -1$,

$$R^{cons}(y, z; y_0, z_0 = 1) = \frac{1}{\sqrt{\pi y}}\Big[\exp\Big[-\frac{(z-1)^2}{y}\Big] + \exp\Big[-\frac{(z+1)^2}{y}\Big]\Big]. \qquad (B5)$$

so that the partial derivative vanishes at $z = 0$ and the parity is even. This solution, given by (3.24), was derived in Sec. III using a Laplace transform.

If, instead, probability is absorbed at $z = 0$ then one may introduce an image source at $z = -1$ so that the probability vanishes at $z = 0$:

$$R^{abs}(y, z; y_0, z_0 = 1) = \frac{1}{\sqrt{\pi y}}\Big[\exp\Big[-\frac{(z-1)^2}{y}\Big] - \exp\Big[-\frac{(z+1)^2}{y}\Big]\Big]. \qquad (B6)$$

This solution (see also eq. (3.25)) has odd parity. For other values of β, the method of images cannot be applied to eq.(B2) since it depends explicitly on z for $\beta \neq 1/2$. However, because of the even character of (B2), it is nonetheless true that the appropriate probability absorbing solution is the odd parity Green's function of (B2):

$$R^{abs}(y, z; y_0, z_0 = 1) = 2\, y^{-1} e^{-(1+z^2)/y}\, z^\beta\, I_{1-\beta}(2z/y). \qquad (B7)$$

We have simply replaced the Bessel function $I_{\beta-1}(2z/y)$ of (3.6) by its linearly independent partner, $I_{1-\beta}(2z/y)$. One may explicitly verify that it satisfies (B2), that it is analytic for all real z and that is is odd in z. In addition, it approaches a delta function as $y \to 0$. This justifies the solution (3.23), which is strictly valid for $0 < \beta < 1$, as the Green's function for absorbing boundary conditions. As discussed in Appendix A, β could take on a continuous range of values from 0 to 1 depending upon how the stochastic noise terms are evaluated. The cases involving integer values, $\beta = 0$ and $\beta = 1$, should be treated as limits, individually as $\beta \to 0$, 1; these were discussed in Sec.III.B.4.

Without the change of variable, (3.6b), it would have been difficult to determine the appropriate Green's function. For example, for the case $\beta = 1/2$, we employed an image source at negative values of z corresponding to imaginary values of ϕ. Needless to say, an imaginary source does not admit a simple physical interpretation.

REFERENCES

[1] Bahcall, N. and Soneira, R., Astrophys. J.**270**, 70 (1983).

[2] De Lapparent, V., Geller, M.J. and Huchra, J.P., Ap. J. **302**, L1 (1986).

[3] Dressler, A., Faber, S.M., Burstein, D., Davies, R.L., Lynden-Bell, D., Terlevich, R.J. and Wegner, G., Astrophys. J. Lett. **313**, L37 (1986).

[4] Maddox, S.J., Efstathiou, G., Sutherland, W.J. and Loveday, J., Mon. Not. R. Astr. Soc., **242**, 43P (1990).

[5] Broadhurst, T.J., Ellis, R.S., Koo, D.C. and Szalay, A.S., preprint submitted to Nature (1989).

[6] Halliwell, J.J. and Hawking, S., Phys. Rev. **D31**, 1777 (1985).

[7] Fischler, W., Ratra, B. and Susskind, L., Nucl. Phys. **B259**, 730 (1985) .

[8] Salopek, D.S, Bond, J.R. and Bardeen, J.M., Phys. Rev. D **40**, 1753 (1989).

[9] Aryal, M. and Vilenkin, A., Phys. Lett. **199B**, 351 (1987).

[10] Starobinski, A.A., in *Current Topics in Field Theory, Quantum Gravity, and Strings*, Proc. Meudon and Paris VI, ed. H.T. de Vega and N. Sanchez **246** 107 (Springer-Verlag, 1986)

[11] Halliwell, J.J., Institute for Theortical Physics Preprint (1988).

[12] Salopek, D.S. and Bond, J.R., submitted to Phys. Rev. D (1990). Referred to as SB1.

[13] Bardeen, J.M. and Bublik, G.J., Class. Quant. Grav. **5**, L113 (1988).

[14] Graziani, F.R. and Olynyk, K.O. Fermilab Pub-85 175-T.

[15] Hosaya, A., Morikawa, M. and Nakayama, K., Intern. Jour. Mod. Phys. A. **4**, 2613 (1989).

[16] Nakao, K., Nambu, Y. and Sasaki, M., Prog. Theor. Phys. **80**, 1041 (1988).

[17] Goncharov, A.S., Linde, A.D. and Mukhanov, V.F., Intern. Jour. Mod. Phys. A. **2**, 561 (1987).

[18] Allen, T.J., Grinstein, B. and Wise, M.B., Phys. Lett. **197B**, 66 (1987).

[19] Kofman, L.A. and Linde, A.D., Nucl. Phys. **B282**, 555 (1987).

[20] Ortolan, A., Lucchin, F. and Matarrese, S., Phys. Rev. **D38**, 465 (1988).

[21] Matarrese, S., Ortolan, A. and Lucchin, F. University of Padua preprint (1989).

[22] Hodges, H.M., Santa Cruz Institute for Particle Physics, preprint, SCIPP-89/01 (1989).

[23] Salopek, D.S., in preparation (1990).

[24] Bond, J.R. and Salopek, D.S., in preparation (1990).

[25] Misner, C., Thorne, K.S. and Wheeler, J.A., *Gravitation*, Freeman (1973).

[26] Bunch, T.S. and Davies, P.C.W., Proc. R. Soc. Lond. A. **360**, 117 (1978).

[27] Bardeen, J.M., Bond, J.R., Kaiser, N. and Szalay, A.S., Ap.J. **304**, 15 (1986).

[28] Bardeen, J.M., Steinhardt, P.J. and Turner, M.S., Phys. Rev. D **28**, 670 (1983).

[29] Bond, J.R. and Efstathiou, G., Astrophys. J. Lett. **285**, L45 (1984).

[30] Bond, J.R., *Distortions and Anisotropies of the Cosmic Background Radiation*, in *The Early Universe*, ed. Unruh, W.G. (Dordrecht:Reidel) (1988).

[31] Lucchin, F. and Matarrese, S., Phys. Rev. **D32**, 1316 (1985).

[32] Sahni, V., Class. Quantum Grav. **5**, L113 (1988).

[33] Ratra, B., Princeton University Preprint (1990).

[34] Abramovitz, M. and Stegun, I.A. *Handbook of Mathematical Functions*, Dover Publications, New York (1972).

[35] Gradsteyn, I.S. and Rhyzhik, I.M., *Table of Integrals, Series and Products* , Academic Press, New York (1980).

[36] van Kampen, N.G., *Stochastic Processes in Physics and Chemistry* , North Holland, Amsterdam (1981).

[37] Vittorio, N., Lucchin, F. and Matarrese, S., Astrophys. J. **328**, 69 (1988).

[38] Chandrasekhar, S., Rev. Mod. Physics, **15**, 1 (1943).

[39] Press, W. H., Flannery, B.P., Teukolsky, S.A. and Vetterling, W.T., *Numerical Recipes* (Cambridge University Press 1986).

[39] Bardeen, J. M., *Proc. CCAST Symposium on Particle Physics and Cosmology*, ed. A. Zee, (New York: Gordon and Breach (1988)).

[40] Kofman, L.A., and Pogosyan, D.Y., Tallinn Preprint (1989).

FIGURE CAPTIONS

Fig. 1: The dispersion in the scalar field for an exponential potential (3.1) with $p = 5$, using the analytic Green's function solution of the Fokker-Planck equation (3.6), is plotted against the initial value of the Hubble parameter, $H(\phi_0)$. The value of $H(\phi_0)$ when our comoving horizon crossed the Hubble radius during inflation determines the microwave background temperature anisotropy dispersion, $\langle(\Delta T_{cmb}/T_{cmb})^2\rangle$, which is roughly proportional to the scalar field dispersion through eq.(3.12b). Current limits on $\Delta T_{cmb}/T_{cmb}$ imply $H(\phi)/m_{\mathcal{P}} \lesssim 10^{-4}$ for the initial condition corresponding to our patch of the Universe.

Fig. 2: Starting with a uniform value of the Hubble parameter consistent with microwave background anisotropy limits, $H(\phi_0) = 10^{-5} m_{\mathcal{P}}$, the probability function $P(\phi|T)$ (3.6) is shown at several times $T = \ln(Ha)$ for an exponential potential with $p = 5$. The width of $P(\phi|T)$ grows as quantum fluctuations cross the Hubble radius during inflation. The horizontal axis has the classical drift subtracted out. The final (large T) distribution of primordial fluctuations (solid curve) is of interest for cosmic structure formation. It moves as a wave with constant width w given by (3.14). All the curves are Gaussian to an excellent approximation, a result independent of the choice of factor ordering in the diffusion equation.

Fig. 3: The same system as in Fig.2, but with $H(\phi_0) = 1.0 m_{\mathcal{P}}$ describing the homogeneous starting conditions for a patch of the Universe. The Ito factor ordering $\beta = 1$ has been assumed. The Fokker-Planck probability function $P(\phi|T)$ given by eq.(3.6) (solid curve) is shown for late times when it moves as a classical wave of constant width. This non-Gaussian distribution has an exponential tail extending to large values of $-\phi$. For comparison, a Gaussian distribution of the same width and dispersion is also shown (dashed curve). High energy density regions are more numerous than the Gaussian case, whereas the opposite is true for low energy density areas. This probability function is not relevant for observable cosmic structures because it describes length scales very much larger than our present horizon volume.

Fig. 4: The operator ordering of the Fokker-Planck equation is not uniquely specified by the stochastic formalism (see eq.(3.4)). For small initial values of the Hubble parameter, $H(\phi_0) \ll m_{\mathcal{P}}$, the various distribution functions $P(\phi|T)$ do not differ appreciably, although they do when $H(\phi_0) \approx m_{\mathcal{P}}$ as we show for the large time limit, $T - T_0 \to \infty$ in this figure. Probability is conserved ($\int P = 1$) except for $\beta = 0$, which has trajectories leaking to $\phi = -\infty$. Note the more extensive tail in the $\beta = 1/2$ case than in the $\beta = 1$ case. Because the scalar field energy density begins at $\sim m_{\mathcal{P}}^4$ is these cases, the stochastic formalism breaks down.

Fig. 5: If the initial value of the Hubble parameter is comparable to the Planck scale, diffusion may be so rapid that some paths may actually reach $\phi = -\infty$ in a finite time. Rather than make these points reflect and turn back as was assumed in Fig. 4, one may simply remove these points from the distribution by imposing absorbing boundary conditions (eqs.(3.22), (3.23)). In this figure, we show the evolution of the Fokker-Planck distribution function $P(\phi|T)$ for $\beta = 1/2$ starting from a unit probability spike at $T = 0$. It reaches a steady state form when $T > 5$. 1/3 of the scalar field trajectories have diffused to $\phi = -\infty$ so only 2/3 of the initial probability remains at late times. The final probability function is still skewed, with a long tail extending to large energy densities. Boundary effects are important for $0 \leq \beta < 1$, but not for $\beta = 1$, our preferred choice.

Fig. 6: In (a), sample Langevin trajectories for a single scalar field moving down an exponential potential are shown as a function of time, $T = \ln(Ha)$. Correlations between the various paths have been neglected and the classical drift has been removed (see eq.(4.3)). The calculations started with the initial value of the Hubble parameter, $H(\phi_0)$, shown, when the comoving scale $k = 10^{-4}\text{Mpc}^{-1}$ left the horizon. Every timestep (here $\Delta T = 0.2$) the scalar field receives a stochastic impulse $\Delta\phi = (\text{gasdev})\, H(\phi)/(2\pi)\, \Delta T^{1/2}$ proportional to the instantaneous value of the Hubble parameter, where (gasdev) is a Gaussian distributed random number with unit variance.[39] The freeze-out of the paths at $T \approx 5$ because H decreases exponentially in ϕ. In

(b), a histogram for the final distribution in the scalar field derived using 50,000 paths for the inflation model of Fig. 2 is compared with the exact solution (3.6) of the Fokker-Planck equation, thus showing the Monte Carlo approach using Langevin trajectories is computationally viable.

Fig. 7 Contour maps of scalar field fluctuations for a two dimensional slice of a 64^3 lattice simulation for an exponential potential stochastic inflation model with $p = 5$. The initial configurations were homogeneous, with $H(\phi_0)/m_p = 10^{-5}$ for (a) and $H(\phi_0) = 1.0m_p$ for (b). The solid contours correspond to -2σ and -1σ deviations from the scalar field mean, (*i.e.*, high energy density regions) and the broken contours correspond to 0, 1, 2σ fluctuations. The mean has been subtracted out. The initial condition for (a) was chosen to yield scalar field fluctuations that lead to structure compatible with current microwave background anisotropy limits; the fluctuations are Gaussian-distributed to high accuracy. (b) is one of the simplest models where non-Gaussian statistics can arise in cosmology. The map is in initial comoving position rather than final physical position and has a uniform value of $H(\phi)e^{\alpha} = e^{T}$, where T is the time at which the slice is viewed. Because fluctuations are much larger than allowed by present microwave background limits, the size of the lattice is much larger than our present horizon size, and as a result this map has no observable consequences. We use this model to illustrate some general techniques which may be applied to more realistic non-Gaussian models involving multiple fields.

Fig. 8 This figure shows only the -2σ contours of the scalar field distribution for the same cases as in Fig.7. In (a), there are 91 points with $\phi < -2\sigma$, which is approximately what is predicted from Gaussian statistics (94). For (b), because of the long tail in Fig. 3, the high energy density areas with negative values of the scalar field are more numerous than in the Gaussian example of (a): there are 192 points with $\phi \leq -2\sigma$. The high energy density regions are also more strongly clustered at a shorter distance scale. In alternative models which could describe our observable Universe, a significant non-Gaussian tail would have an important impact on structure formation.

Fig. 9 As a check of the numerical method, the final scalar field distributions from the lattice simulations of Fig.7a,b (solid histogram) are shown to agree with the exact solutions of eq.(3.6) with $\beta = 1$ (dashed curves). For (a), with $H(\phi_0) = 10^{-5}m_p$, this is a Gaussian distribution. In (b), of the initially $64^2 = 4086$ points, 22 paths wandered beyond χ_{cut}, eq.(4.6), and were discarded, as described in Sec. IV. Simulations with even larger $H(\phi_0)$ have a much larger loss of trajectories: *e.g.*, with $H(\phi_0) = 3m_p$, approximately 10% of the points are discarded. In single scalar field models, significant non-Gaussian distributions are generated only if the scalar field begins with a Hubble parameter $H(\phi_0) \approx m_p$, corresponding to a patch of the Universe $\approx 10^{20}$ times larger than our observable patch.

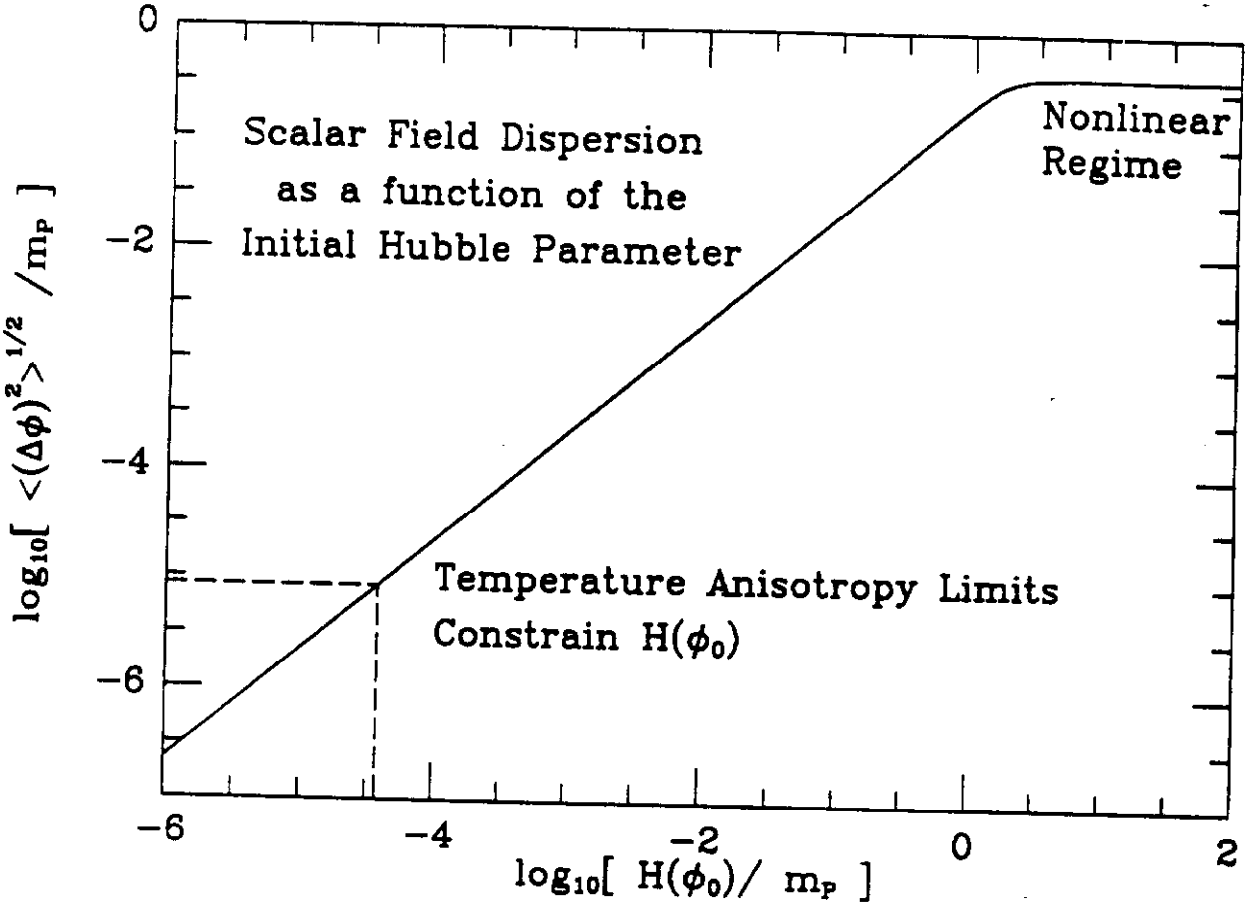
Scalar Field Dispersion
as a function of the
Initial Hubble Parameter
Nonlinear
Regime
Temperature Anisotropy Limits
Constrain H(φ0)
log10[<(Δφ)²>^1/2 /mP]
log10[H(φ0)/ mP]
0
−2
−4
−6
−6
−4
−2
0
2

Fig. 1

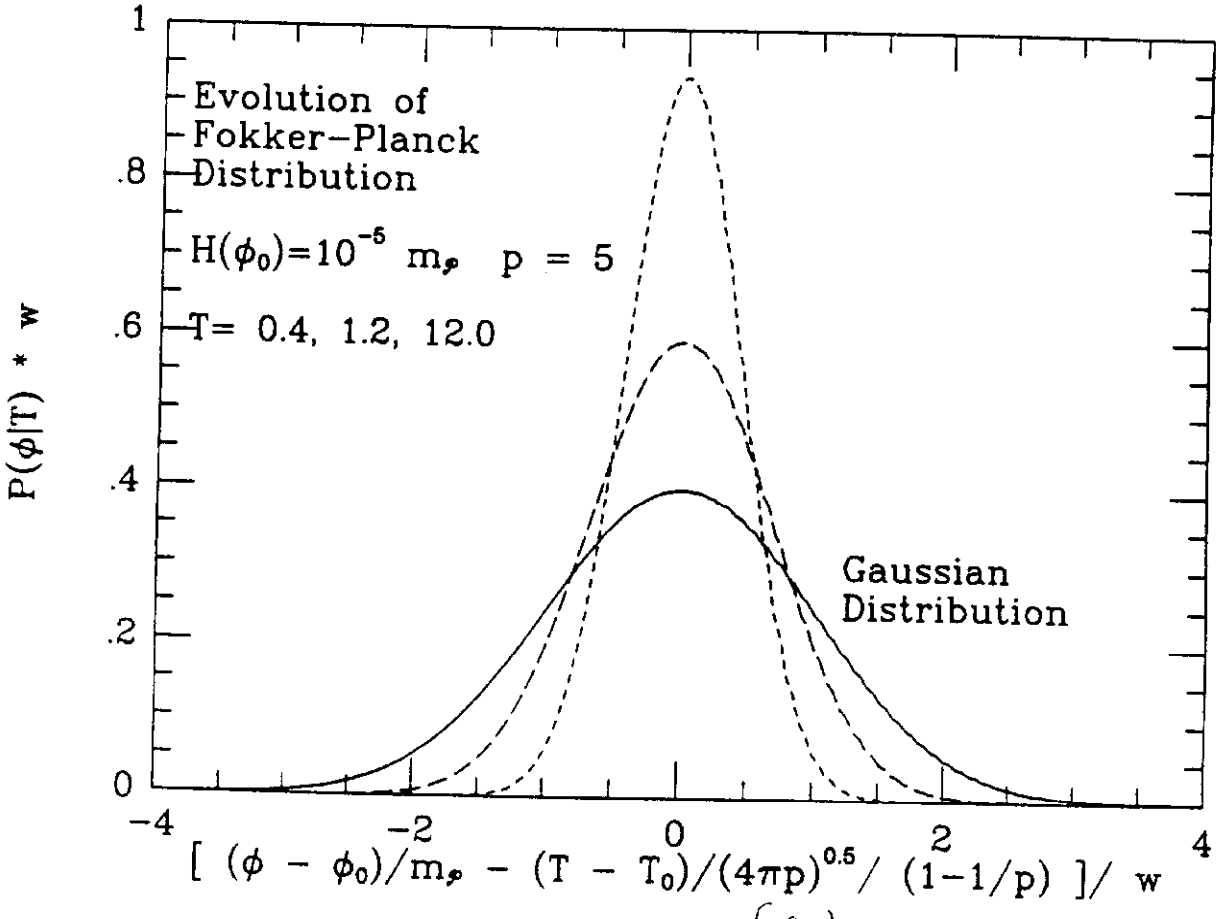
Evolution of
Fokker−Planck
Distribution
H(φ0)=10^-5 mφ p = 5
T= 0.4, 1.2, 12.0
Gaussian
Distribution
P(φ|T) * w
[(φ − φ0)/mφ − (T − T0)/(4πp)^0.5/ (1−1/p)]/ w
1
.8
.6
.4
.2
0
−4
−2
0
2
4

Fig 2

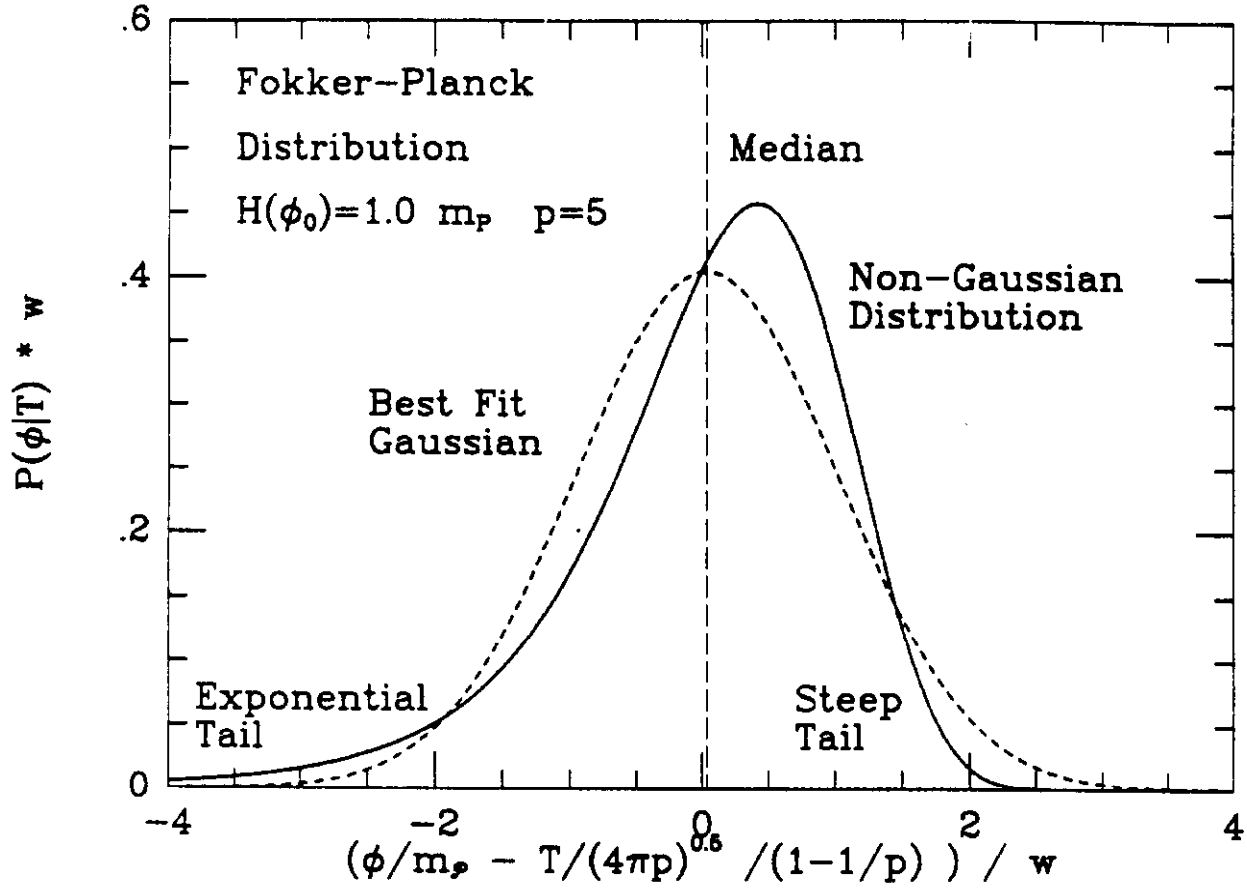
Fokker–Planck
Distribution
H(φ0)=1.0 mp p=5
Median
Non–Gaussian
Distribution
Best Fit
Gaussian
Exponential
Tail
Steep
Tail
P(φ|T) * w
.6
.4
.2
0
−4
−2
0
2
4
(φ/mφ − T/(4πp)^0.5 /(1−1/p))^2 / w

Fig. 3

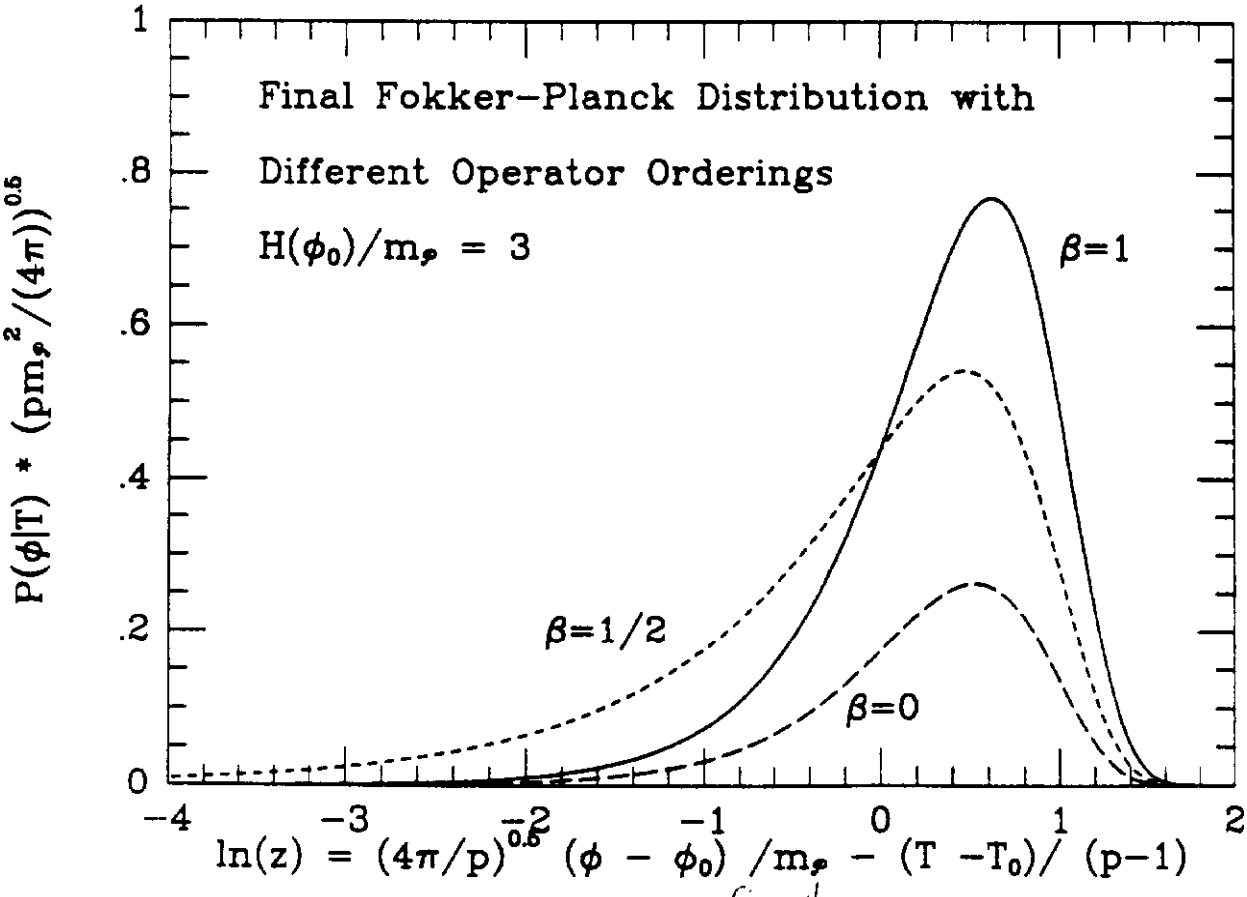
Final Fokker–Planck Distribution with
Different Operator Orderings
H(φ0)/mφ = 3
β=1
β=1/2
β=0
P(φ|T) * (pmφ^2/(4π))^0.5
1
.8
.6
.4
.2
0
−4
−3
−2
−1
0
1
2
ln(z) = (4π/p)^0.5 (φ − φ0) /mφ − (T −T0)/ (p−1)

fig. 4

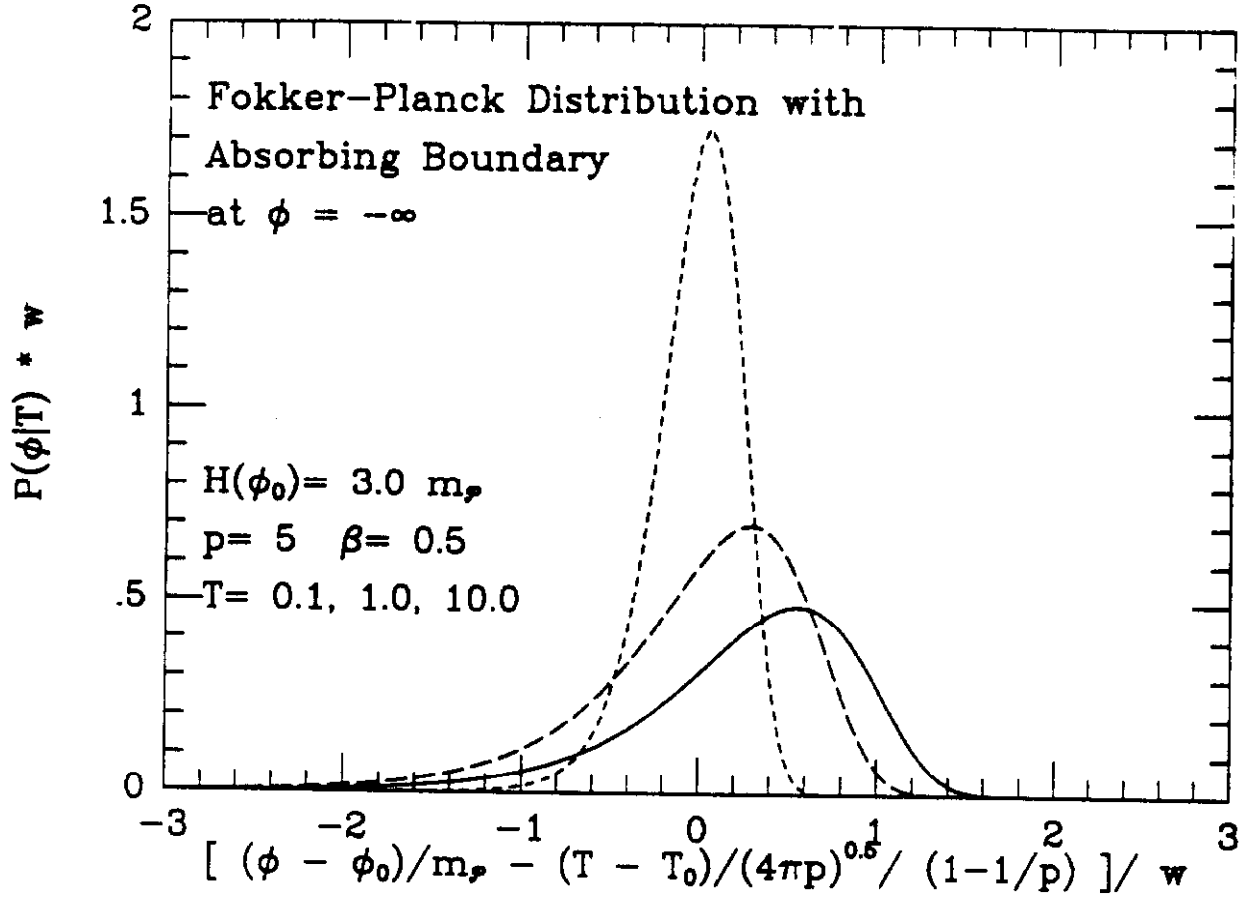
Fokker–Planck Distribution with
Absorbing Boundary
at $\phi = -\infty$
$H(\phi_0)$= 3.0 m_ϕ
p= 5 β= 0.5
T= 0.1, 1.0, 10.0
$P(\phi|T) * w$
$[(\phi - \phi_0)/m_\phi - (T - T_0)/(4\pi p)^{0.5} / (1-1/p)] / w$

Fig.5

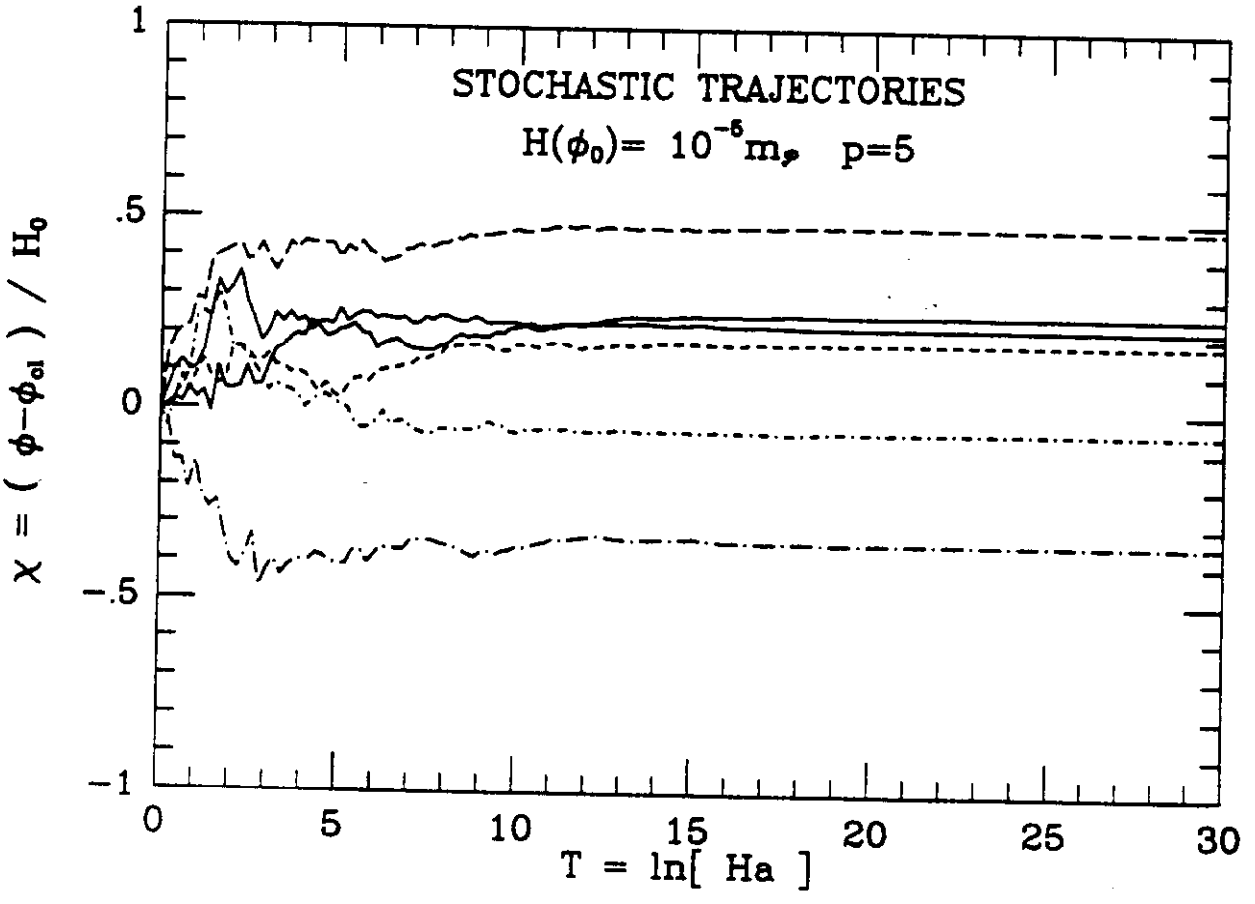
STOCHASTIC TRAJECTORIES
$H(\phi_0)= 10^{-5} m_\phi$ p=5
$\chi = (\phi - \phi_{cl}) / H_0$
T = ln[Ha]

Fig.6

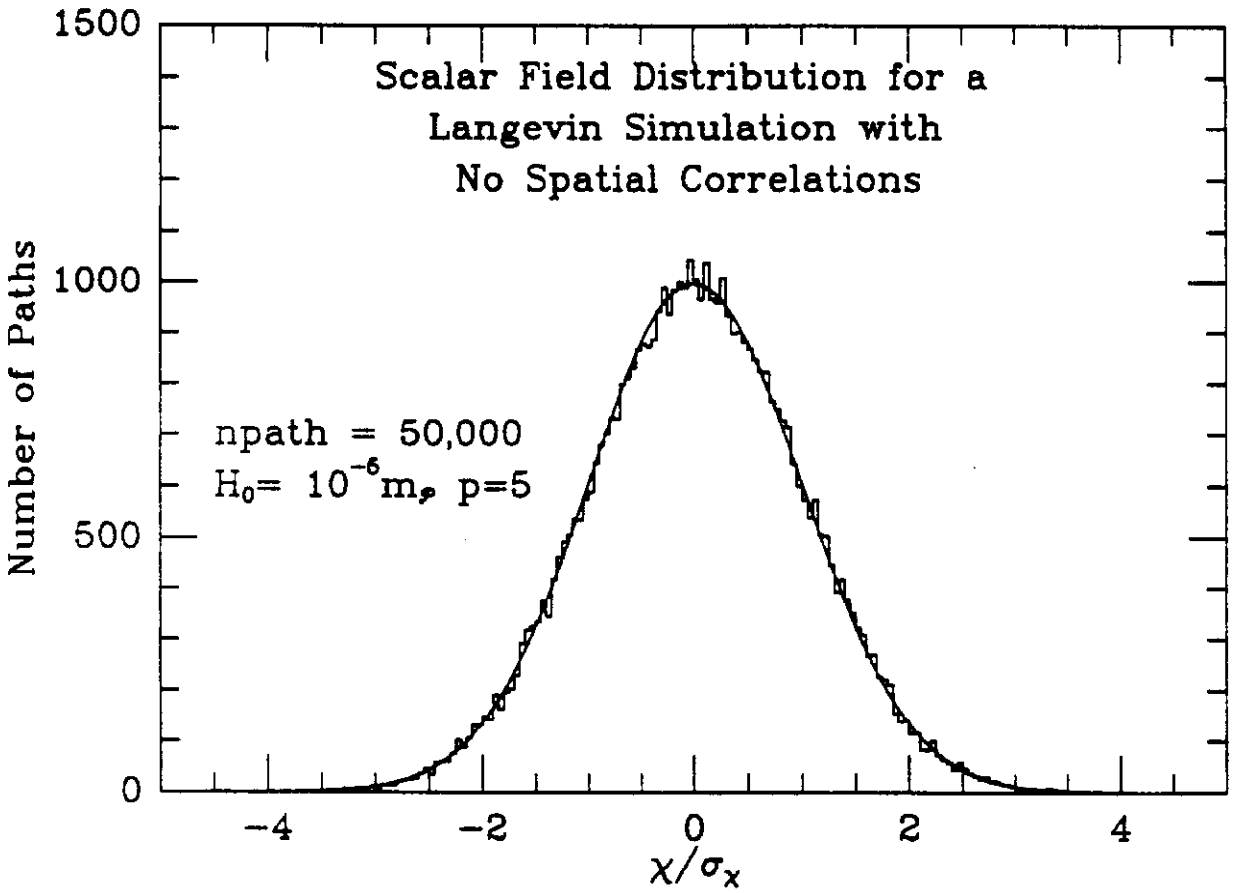
Scalar Field Distribution for a
Langevin Simulation with
No Spatial Correlations
npath = 50,000
$H_0 = 10^{-6} m_\varphi$ p=5
Number of Paths
1500
1000
500
0
−4
−2
0
2
4
χ/σ_χ

Fig. 6b

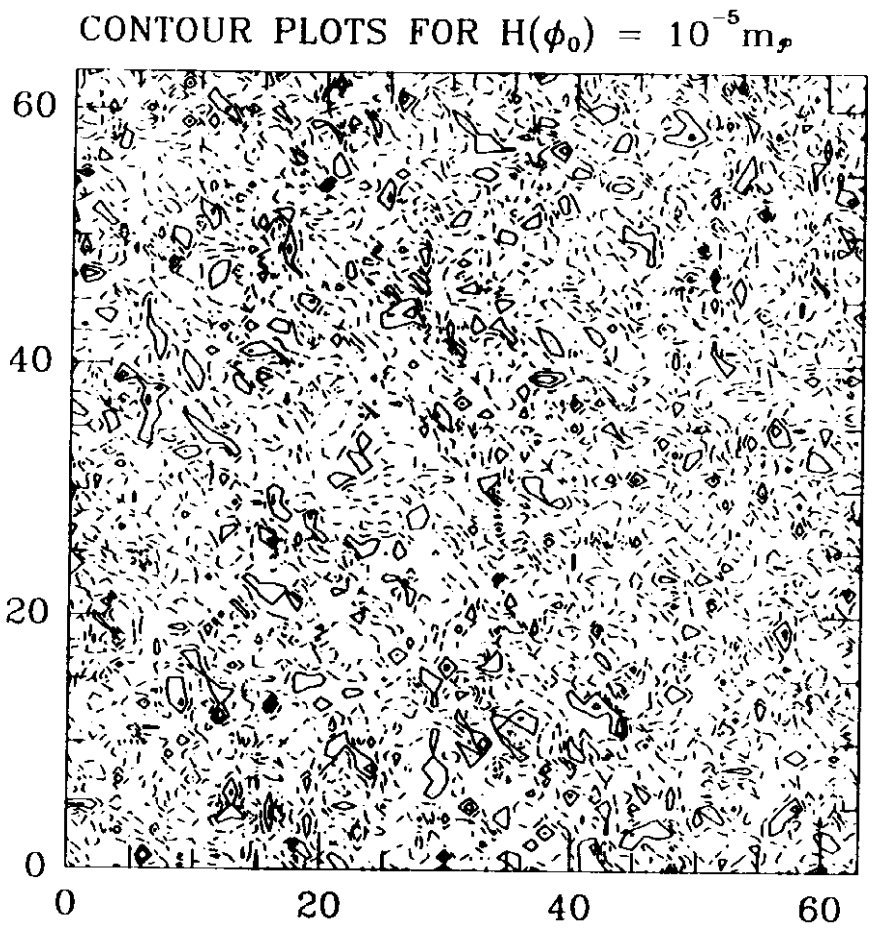
CONTOUR PLOTS FOR H(ϕ_0) = $10^{-5}m_\varphi$
60
40
20
0
0
20
40
60

Fig. 7a

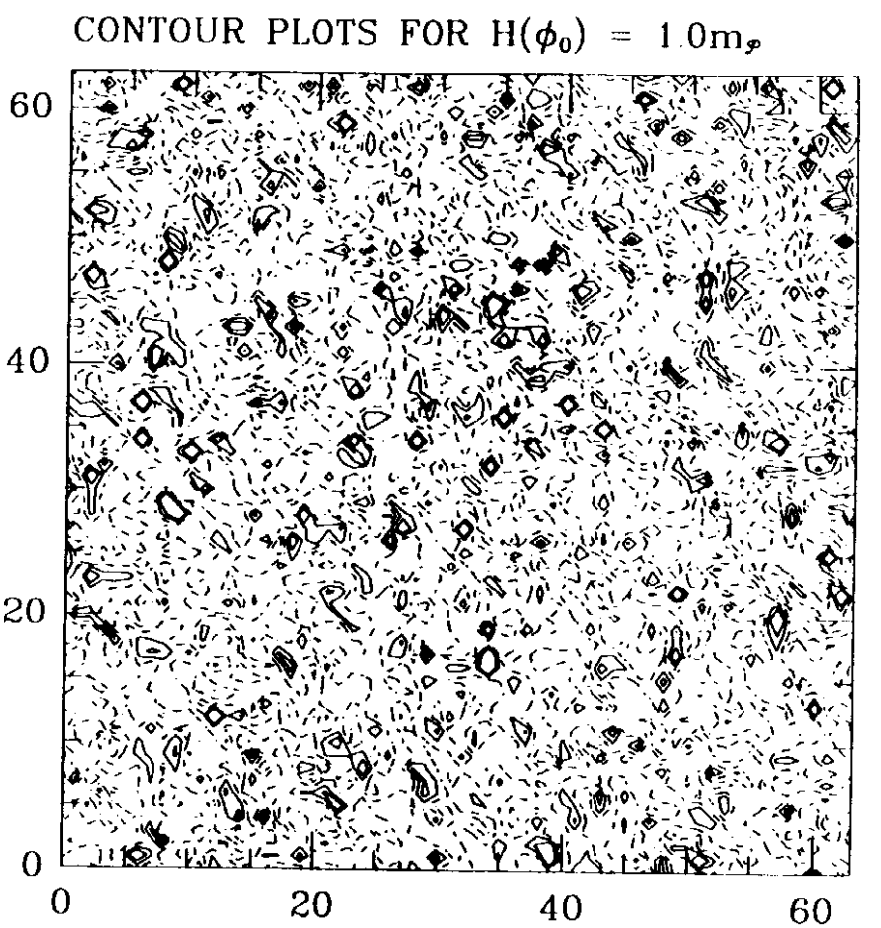
CONTOUR PLOTS FOR H(ϕ_0) = $1.0m_\varphi$
60
40
20
0
0
20
40
60

Fig. 7b

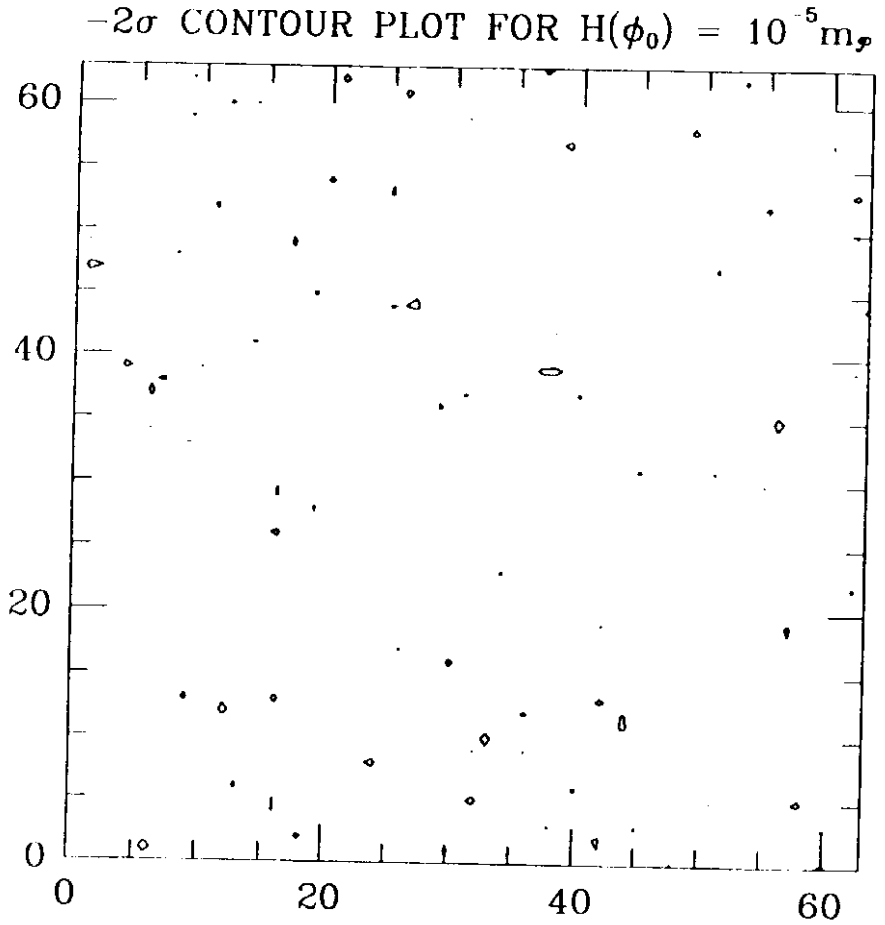
-2σ CONTOUR PLOT FOR $H(\phi_0) = 10^{-5} m_p$
60
40
20
0
0
20
40
60

Fig. 8a

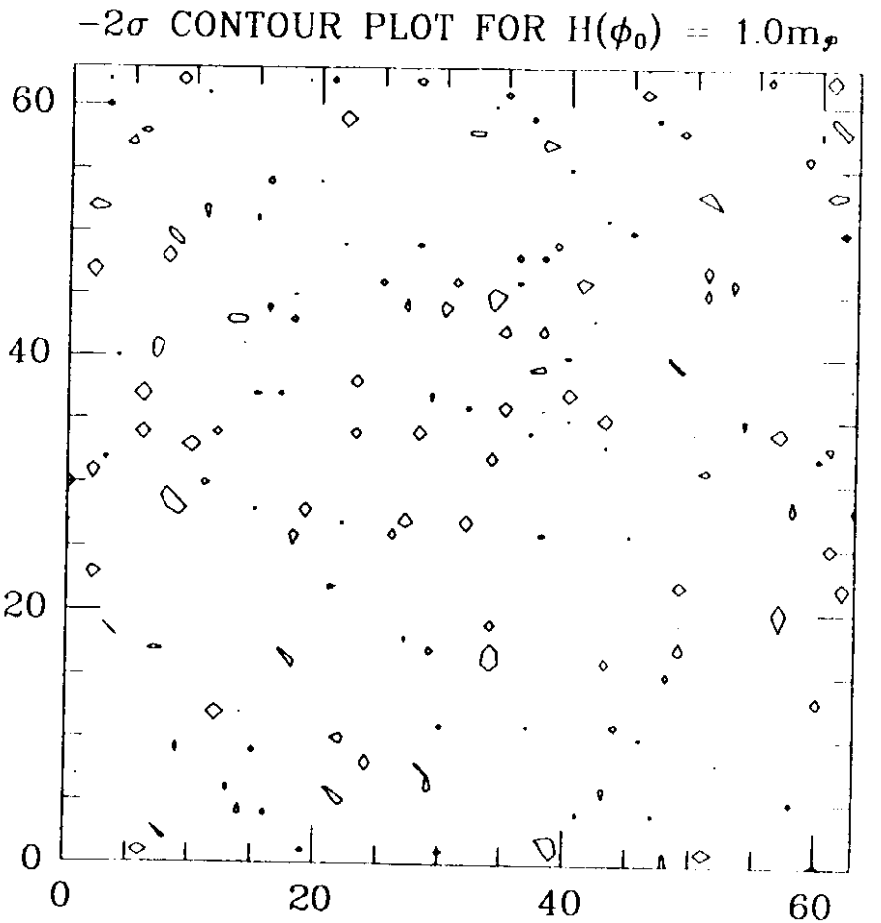
-2σ CONTOUR PLOT FOR $H(\phi_0) = 1.0 m_p$
60
40
20
0
0
20
40
60

Fig. 8b

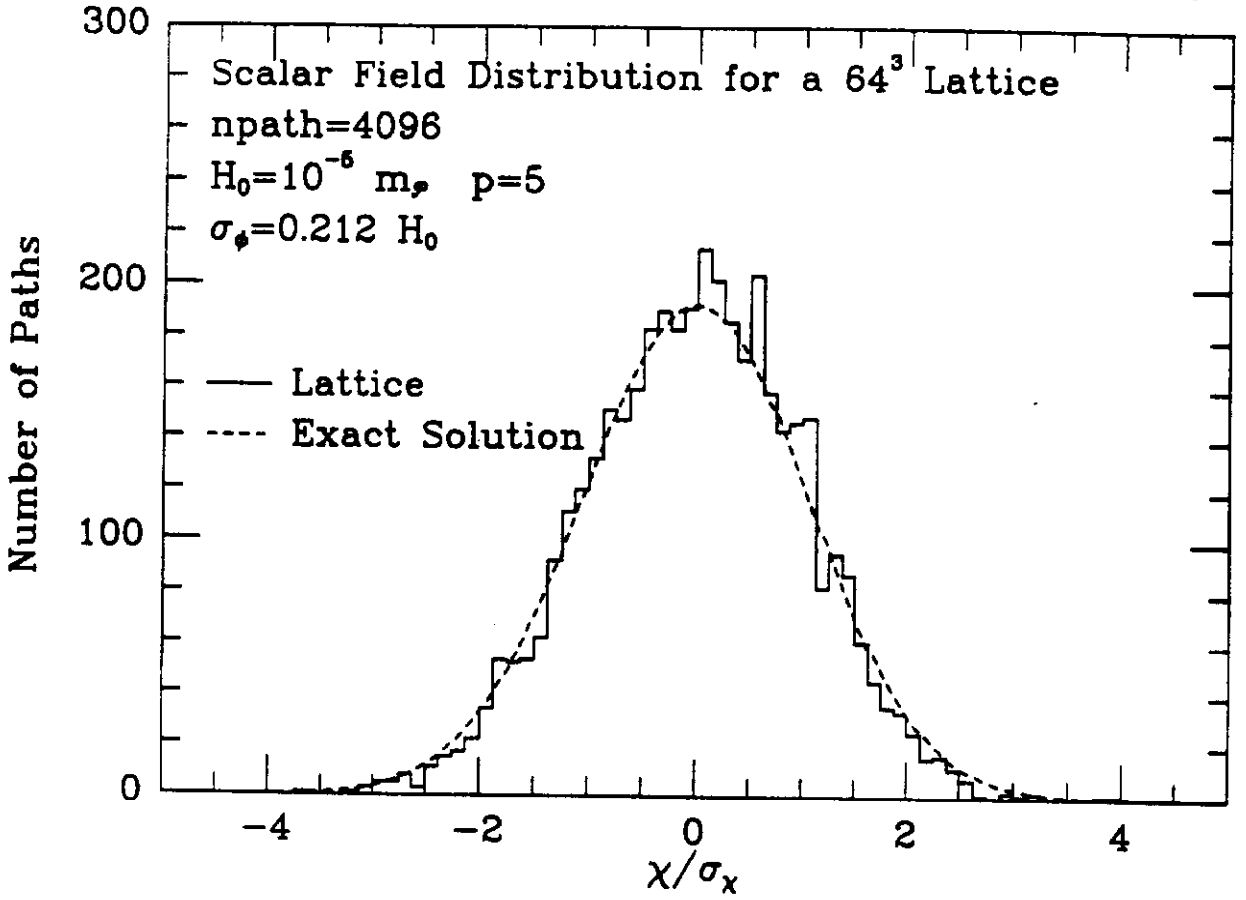
Scalar Field Distribution for a 64^3 Lattice
npath=4096
$H_0=10^{-5}$ m_ϕ p=5
$\sigma_\phi=0.212$ H_0
Lattice
Exact Solution
Number of Paths
300
200
100
0
−4
−2
0
2
4
χ/σ_χ

Fig. 9a

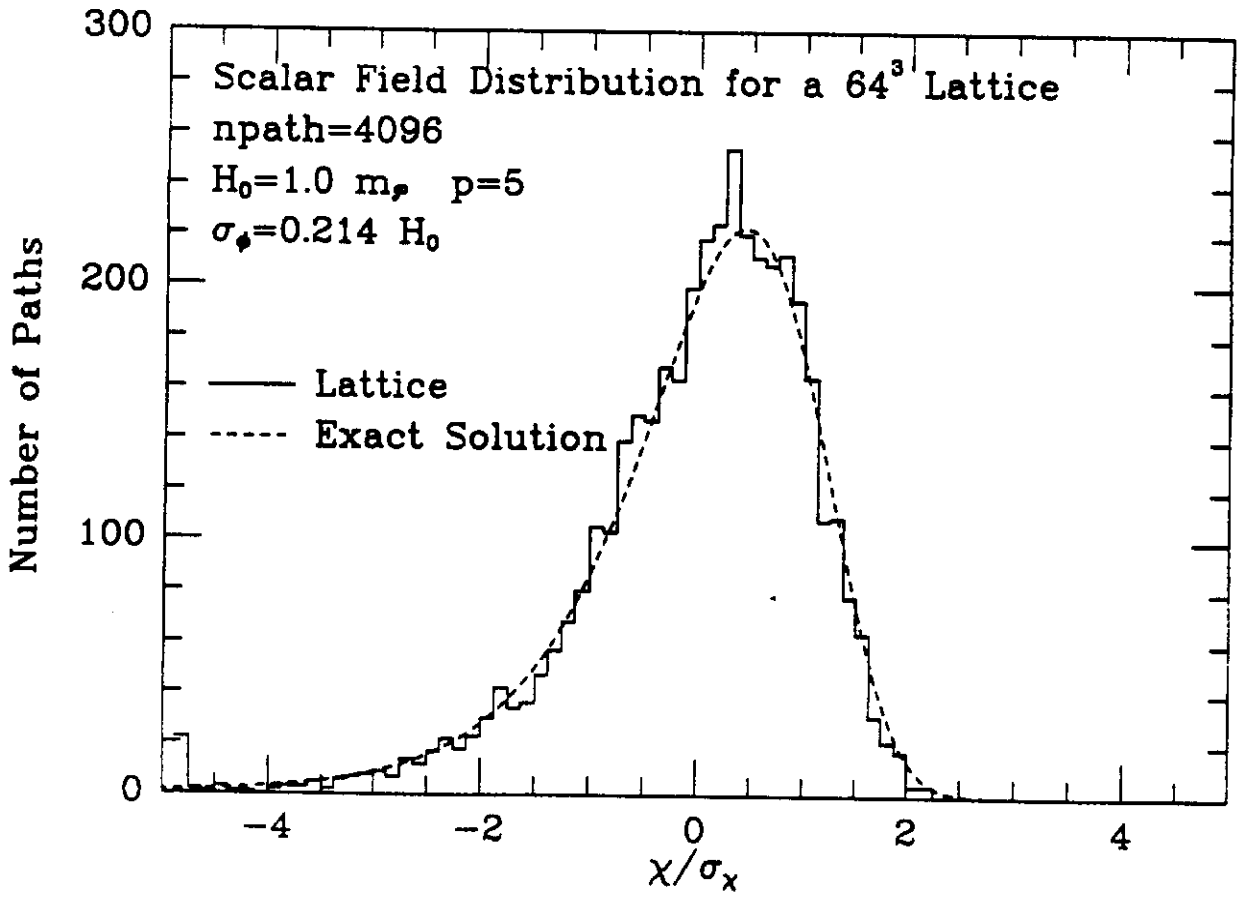
Scalar Field Distribution for a 64^3 Lattice
npath=4096
$H_0=1.0$ m_ϕ p=5
$\sigma_\phi=0.214$ H_0
Lattice
Exact Solution
Number of Paths
300
200
100
0
−4
−2
0
2
4
χ/σ_χ

Fig. 8c